

·专题研究·

伊宁地块特克斯达坂晚石炭世伊什基里克组 双峰式火山岩地球化学特征

宁文涛¹, 李永军^{1,2}, 汪振宇¹, 王祚鹏¹, 李甘雨¹

(1. 长安大学 地球科学与资源学院, 陕西 西安 710054; 2. 自然资源部 岩浆作用成矿与找矿重点实验室,
陕西 西安 710054)

摘要: 伊宁地块特克斯达坂一带出露的晚石炭世伊什基里克组双峰式火山岩主要由玄武岩、流纹岩两大端员组成, 其 SiO_2 含量为 47.13% ~ 77.72%, 在 53.62% ~ 72.15% 之间存在明显的间断, 具有双峰式火山岩的特征。LA-ICP-MS 锆石 U-Pb 定年获得流纹岩年龄为 302.8 ± 3.6 Ma, 表明该套火山岩形成于晚石炭世。玄武岩 SiO_2 含量为 47.13% ~ 53.62%, 具有低 SiO_2 、高 $\text{Fe}_{\text{2}}\text{O}_3$ ($\text{TFe}_{\text{2}}\text{O}_3 = 10.90\% \sim 17.40\%$)、高 MgO ($3.74\% \sim 10.12\%$, 平均为 6.48%) 和高 Na ($\text{Na}_2\text{O} = 2.84\% \sim 6.69\%$)、低 K ($\text{K}_2\text{O} = 0.48\% \sim 3.77\%$) 特征 ($\text{Na}_2\text{O}/\text{K}_2\text{O} = 1.21 \sim 12.18$), 轻稀土元素富集而重稀土元素亏损 [$(\text{La/Yb})_{\text{N}} = 1.58 \sim 4.94$], 具有弱的负 Eu 异常 ($\delta\text{Eu} = 0.30 \sim 1.10$), 亏损 Ta、Nb、Th、Sr 等不相容元素。流纹岩 SiO_2 含量为 72.15% ~ 77.72%, 具有高 SiO_2 、高 K ($\text{K}_2\text{O} = 6.12\% \sim 9.48\%$)、低 Na ($\text{Na}_2\text{O} = 0.40\% \sim 2.39\%$) 特征 ($\text{Na}_2\text{O}/\text{K}_2\text{O} = 0.04 \sim 0.36$), K、Rb 和 LREE 显著富集 [$(\text{La/Yb})_{\text{N}} = 2.46 \sim 10.48$], 相对亏损 Ba、Sr、P、Ti, 且有基本一致的强负 Eu 异常 ($\delta\text{Eu} = -0.18 \sim -0.44$), 具有 A2 型花岗岩地球化学特征。此外, 玄武岩具有相对高的 $\text{Mg}^{\#}$ 值和 Co、Cr、Ni 含量, 其 $\varepsilon\text{Nd}(t)$ 值为 3.45、3.55, 表明玄武岩来自于亏损地幔的部分熔融; 而流纹岩具有低 $\text{Mg}^{\#}$ 和正 $\varepsilon\text{Hf}(t)$ 值, 暗示其形成与玄武质岩浆底侵过程中的地壳熔融有关。结合二阶段锆石 Hf 模式年龄, 认为源区可能与元古宙的变质结晶基底重熔有关。根据上述地球化学特征并结合构造判别图解, 认为特克斯达坂一带伊什基里克组双峰式火山岩形成于造山后伸展环境, 具有板内成因特征。该套典型双峰式火山岩的发现为进一步探讨伊宁地块石炭纪构造演化提供了重要依据。

关键词: 双峰式火山岩; 地球化学特征; 伊什基里克组; 特克斯达坂; 伊宁地块

中图分类号: P588.14; P597

文献标识码: A

文章编号: 1000-6524(2019)01-0001-20

Geochemical characteristics of the bimodal volcanic rocks in Upper Carboniferous Yishijilike Formation in Tekes Daban area of Yining landmass

NING Wen-tao¹, LI Yong-jun^{1,2}, WANG Zhen-yu¹, WANG Zuo-peng¹ and LI Gan-yu¹

(1. School of Earth Science and Resources, Chang'an University, Xi'an 710054, China; 2. Key Laboratory for the Study of Focused Magmatism and Giant Ore Deposits, MNR, Xi'an 710054, China)

Abstract: The bimodal volcanic rocks of Upper Carboniferous Yishijilike Formation from the Tekes Daban area in Yining landmass consist mainly of basalts and rhyolites. Their SiO_2 values range from 47.13% to 77.72%, and exhibit a gap of SiO_2 between 53.62% and 72.15%, displaying a typical bimodal geochemical affinity. The LA-ICP-MS zircon U-Pb ages of rhyolites yielded an age of 302.8 ± 3.6 Ma, suggesting that these bimodal volcanic rocks

收稿日期: 2017-10-22; 接受日期: 2018-11-05; 编辑: 郝艳丽

基金项目: 国家自然科学基金项目(41273033, 41303027)

作者简介: 宁文涛(1993-), 男, 硕士研究生, 构造地质学专业, E-mail: 18717333531@163.com; 通讯作者: 李永军(1961-), 男, 教授, 博士生导师, 从事构造地质学、区域地质调查研究, E-mail: yongjunl@chd.edu.cn。

网络首发时间: 2018-12-11; 网络首发地址: <http://kns.cnki.net/kcms/detail/11.1966.P.20181207.1734.004.html>

were formed at the beginning of Late Carboniferous. Basalt samples have SiO_2 values of 47.13% ~ 53.62%, with high Fe_2O_3 (TFe_2O_3 being 10.90% ~ 17.40%) and MgO (3.74% ~ 10.12%, 6.48% on average), high Na (2.84% ~ 6.69%) and low K (0.48% ~ 3.77%) values. The basalts are obviously enriched in light rare earth elements and depleted in heavy rare earth elements [$(\text{La/Yb})_N = 1.58 \sim 4.94$]. In contrast, the rhyolites samples have SiO_2 values of 72.15% ~ 77.72%, high K (6.12% ~ 9.48%) and low Na (0.40% ~ 2.39%) concentrations. Compared with the basalts of bimodal volcanic rocks, they show significant depletion of Ba, Sr, P, Ti elements, obvious enrichment of light rare earth elements and relative depletion of heavy rare earth elements. They exhibit strongly negative Eu anomaly ($\delta\text{Eu} = 0.18 \sim 0.44$) and geochemical characteristics of A2 type granites. In addition, the basalts have high values of $\text{Mg}^{\#}$, Co, Cr, Ni, with $\varepsilon\text{Nd}(t)$ of basalt samples being 3.45 and 3.55. These features indicate that basaltic magmas were derived from partial melting of a depleted mantle source. The rhyolites of the Yishkilike Formation have low $\text{Mg}^{\#}$ and positive $\varepsilon\text{Hf}(t)$ values, suggesting that their formation was related to crustal melting during the process of basaltic magma underplating. Combined with the two-stage Hf model ages, it is suggested that the rhyolite source may be related to the reworking of Proterozoic metamorphic basement. These geochemical characteristics together with structural tectonic discriminant diagrams show that the bimodal volcanic rocks of the Yishijilike Formation were formed in a post-orogenic extensional environment with intraplate genetic characteristics. The discovery of the typical bimodal volcanic rocks provides important information for further study of the Carboniferous tectonic evolution in Yining landmass.

Key words: bimodal volcanic rocks; geochemical characteristics; Yishijilike Formation; Tekes Daban; Yining landmass

Fund support: National Natural Science Foundation of China (41273033, 41303027)

天山造山带位于中亚造山带西南缘(图1a),由一系列古生代岛弧、蛇绿岩套、增生楔、大洋高原和微板块等俯冲增生型块体组成(Windley *et al.*, 1990; Allen *et al.*, 1993; Gao *et al.*, 1998; Xiao *et al.*, 2004)。处于天山造山带腹地的伊宁地块主要出露两套石炭纪火山岩,即早石炭世大哈拉军山组和晚石炭世伊什基里克组火山岩。大哈拉军山组火山岩出露面积最广,主体为钙碱性火山沉积建造,主要于伊宁地块南北缘及地块内部分布。伊什基里克组在伊宁地块分布有限,主要集中于伊宁市以北博罗科努南麓与东部阿吾拉勒一带,乌孙山地区小面出露。长久以来,学者们对这两套火山岩的构造属性分歧较大。主流观点认为,大哈拉军山组火山岩产于与弧环境有关的俯冲环境(Gao *et al.*, 1998; 朱永峰等, 2006; 钱青等, 2006; Wang *et al.*, 2007; 唐功建等, 2009; 李永军等, 2012, 2018; An *et al.*, 2013; 李大鹏等, 2013; 韩琼等, 2015; 汪帮耀等, 2016),而伊什基里克组火山岩被认为是天山洋盆完成俯冲碰撞造山后的陆内拉张环境火山产物,主体为一套特征明显的双峰式火山岩组合(李永军等, 2017)。但是关于这套双峰式火山岩详细的野外地质特征、岩石学、地球化学、年代学和同位素资料鲜

有报道,使得部分学者认为伊宁地块晚石炭世仍处于与弧有关的俯冲环境(Tang *et al.*, 2014; Yin *et al.*, 2017),因此关于晚石炭世双峰式火山岩的报道显得尤为重要。

笔者通过野外地质调查发现伊宁地块特克斯达坂一带存在典型的晚石炭世双峰式火山岩组合。本套火山岩露头尺度呈明显的基性、酸性两个端员系列频繁交替出现,接触界限截然,既有宽双峰式产出,局地又表现为窄双峰式韵律,是区内目前发现的最有代表性的双峰式火山岩组合。本文从野外宏观地质特征、岩石学、年代学、地球化学等方面对其进行研究,详细讨论了本套火山岩的岩石成因及产出环境,以进一步为伊宁地块石炭纪构造演化提供重要依据。

1 地质概况及岩石学特征

伊宁地块自西向东呈楔形尖灭,南北各有古生代叠加岛弧带与准噶尔板块和塔里木板块相隔。这里要说明的是,本文所述的伊宁地块,不同于前人所述的 Yili Block (Wang *et al.*, 2006, 2008, 2009) 或 Yili-Central Tianshan (Gao *et al.*, 1998; 高俊等,

2009),而是将前人划分的 Yili Block 剔出北部博罗科努构造带后所剩下的区域(图 1b)(李永军等,2017)。

石炭系是伊宁地块的主体,分布最广,是记录该地块形成、演化与消亡的关键地层。区内石炭系自

下而上依次为早石炭世大哈拉军山组火山岩、阿克沙克组碎屑岩与碳酸盐岩、晚石炭世伊什基里克组双峰式火山岩、东图津河组碎屑岩和科古琴山组碎屑岩,各组之间均以角度不整合接触(李永军等,2008a)。

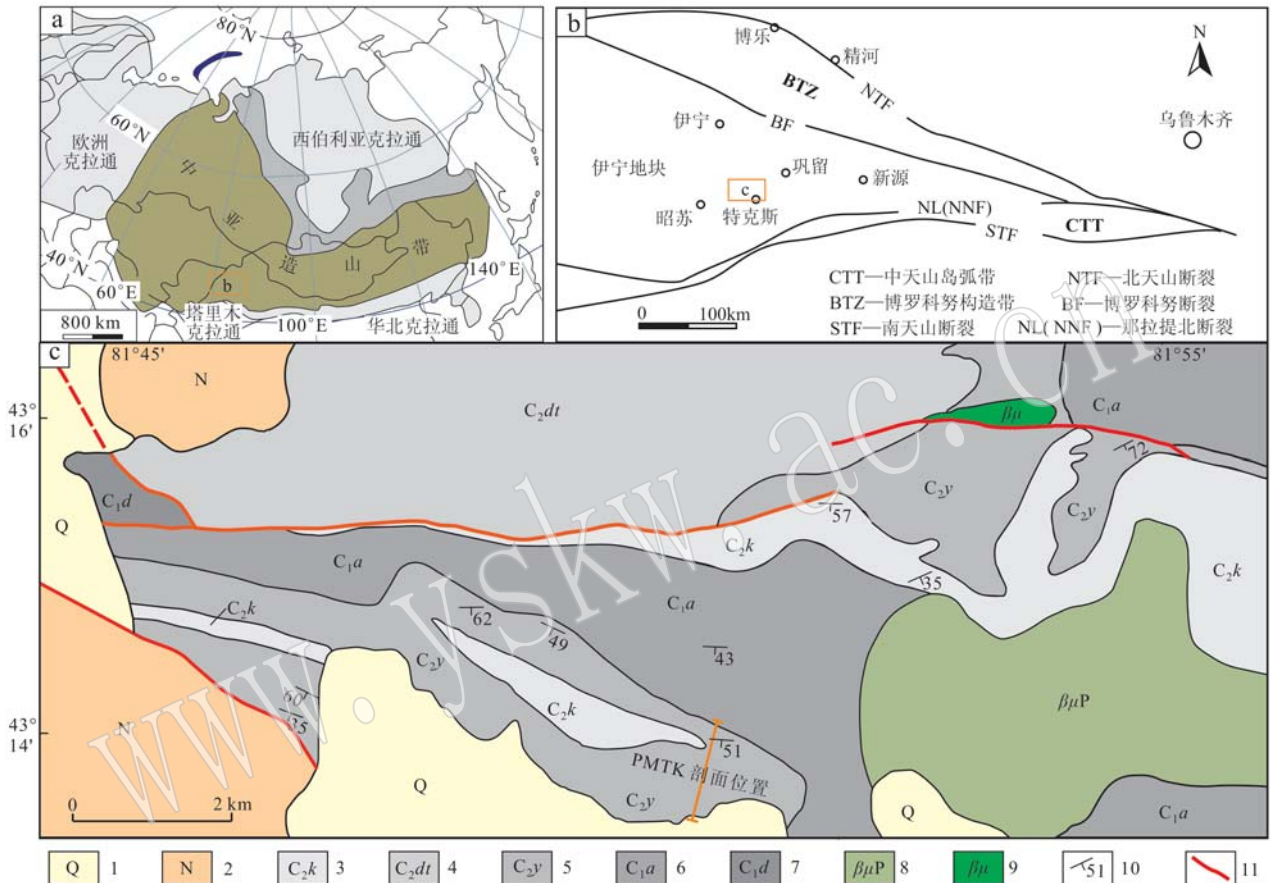


图 1 伊宁地块特克斯达坂一带地质简图

Fig. 1 Geological sketch map of Tekes Daban area in Yining landmass

a—中亚造山带构造位置示意图(据 Jahn et al., 2000); b—伊宁地块构造位置示意图(据李永军等,2017); c—特克斯达坂一带地质简图; 1—第四系; 2—新近系; 3—上石炭统科古琴山组; 4—上石炭统东图津河组; 5—上石炭统伊什基里克组; 6—下石炭统阿克沙克组; 7—下石炭统大哈拉军山组; 8—二叠系基性岩体; 9—基性岩体; 10—产状; 11—断层

a—simplified tectonic sketch map of the Central Asian Orogenic Belt (after Jahn et al., 2000); b—simplified tectonic sketch map of Yining landmass (after Li Yongjun et al., 2017); c—geological sketch map of Tekes Daban, Xinjiang; 1—Quaternary; 2—Neogene; 3—Upper Carboniferous Keguinshan Formation; 4—Upper Carboniferous Dongtujinhe Formation; 5—Upper Carboniferous Yishijilike Formation; 6—Lower Carboniferous Akeshake Formation; 7—Lower Carboniferous Dahalajunshan Formation; 8—Permian basic rocks; 9—basic rocks; 10—attitude; 11—fault

特克斯达坂一带的伊什基里克组由 PMTK 剖面控制(图 1c),该组整体为南倾单斜地层(图 2),并与下伏阿克沙克组呈角度不整合接触。组内主要由火山熔岩和火山碎屑岩组成,总厚度为 1 325.17 m。其中,伊什基里克组双峰式火山岩在 PMTK 剖面的 18 与 24 层出露明显,基、酸两个端员交替产出(未见中性端员),两个端员成分差异显著,颜色红黑相间,

接触界限截然,由 PMSF1 与 PMSF2 剖面进一步控制(图 2)。

双峰式火山岩主要由灰黑色玄武岩、肉红色流纹岩组成。玄武岩为斑状结构,块状构造(图 3a、3b),斑晶(10%)由斜长石、辉石组成(图 3c、3d),其中斜长石多呈半自形-自形板状,聚片双晶发育;基质约 90%,由斜长石和玻璃质组成,斜长石(35%)

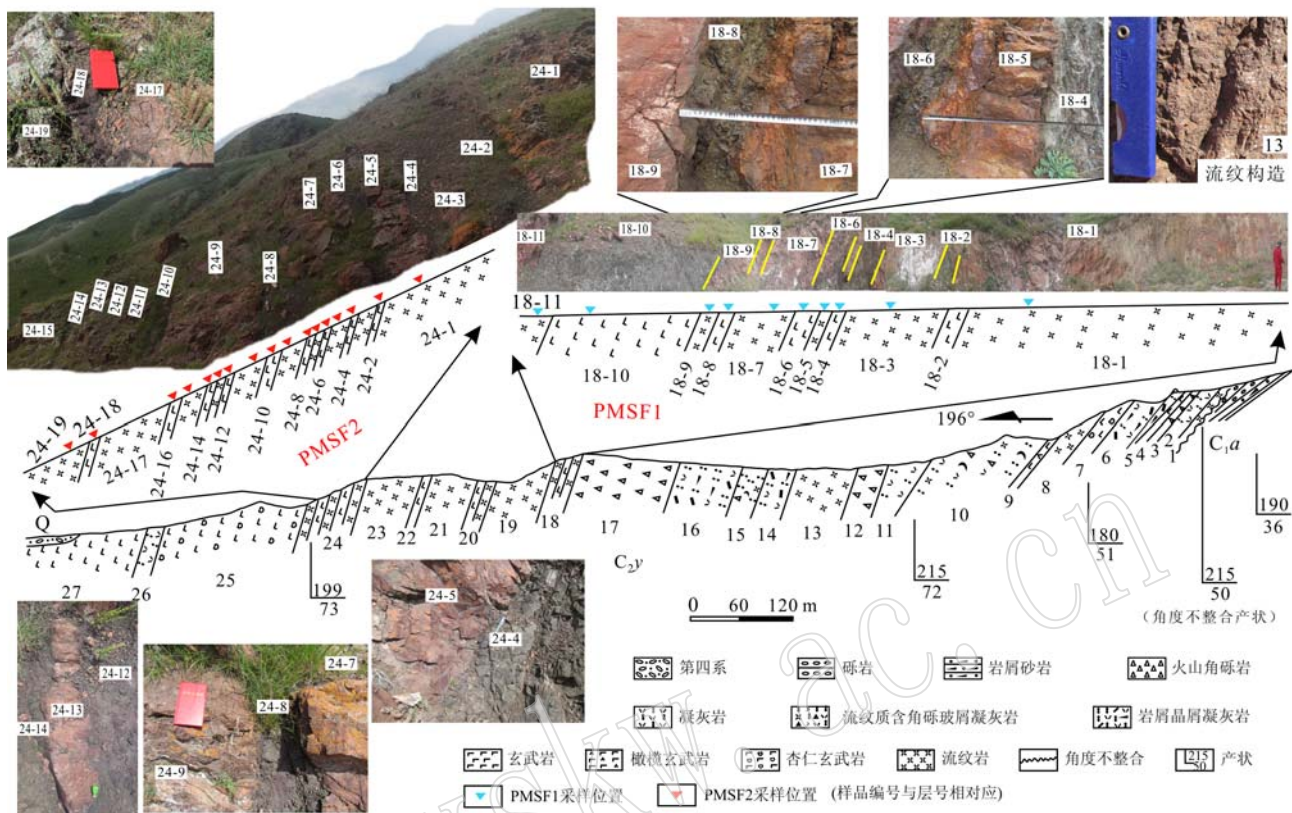


图2 特克斯达坂一带伊什基里克组实测地质剖面图及样品位置
Fig. 2 Geological section of Yishijilike Formation in Tekes Daban and location of the sample

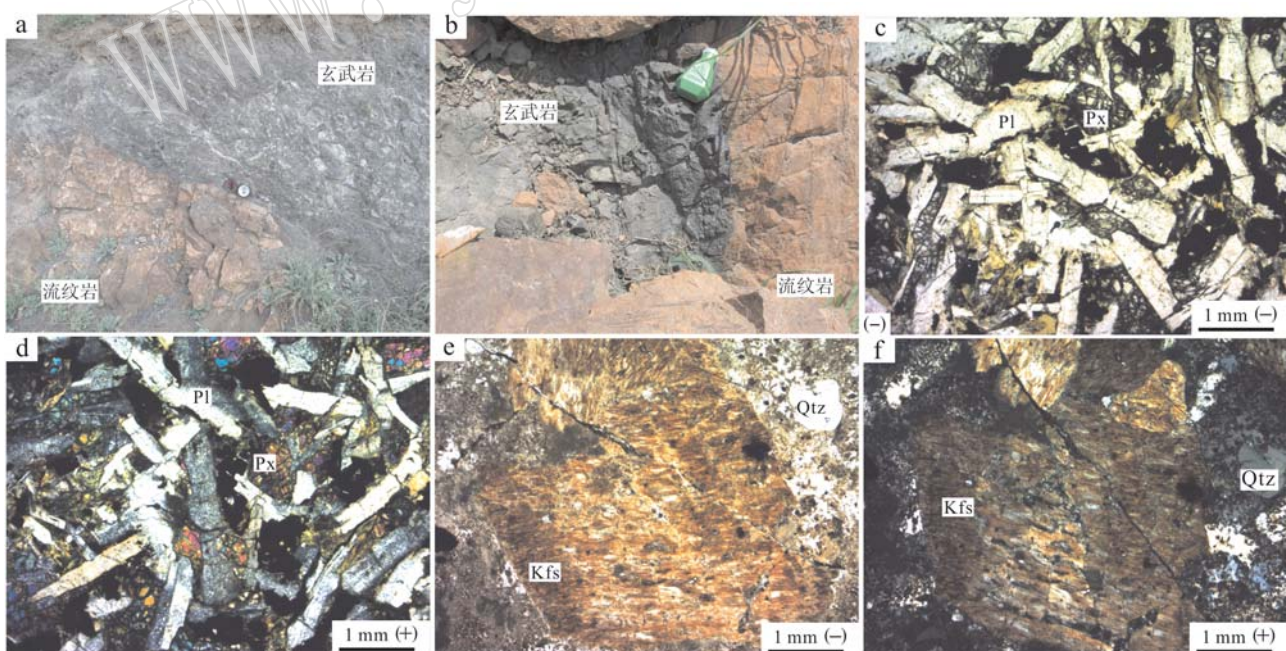


图3 伊什基里克组玄武岩、流纹岩野外(a,b)及镜下特征(c,d,e,f)照片
Fig. 3 Macroscopic (a, b) and microscopic (c, d, e, f) photos of basalts and rhyolite from Yishijilike Formation
a, b—玄武岩与流纹岩野外照片; c, e—玄武岩单偏光显微镜照片; d, f—玄武岩与流纹岩正交偏光显微镜照片
Pl—斜长石; Px—辉石; Kfs—钾长石; Qtz—石英
a, b—species of rocks; c, e—plainlight photos of basalt and rhyolite; d, f—crossed nicols photos of basalt and rhyolite;
Pl—plagioclase; Px—pyroxene; Kfs—K feldspar; Qtz—quartz

呈半自形-自形细板条状,相互交错,搭成格架,其间充填玻璃质,玻璃质(50%)已全部脱玻蚀变为绿泥石和碳酸盐。流纹岩为斑状结构,块状构造(图3a、3b),斑晶含量约18%,由石英和钾长石组成(图3e、3f),钾长石(6%)半自形板-他形粒状,石英(12%)溶蚀呈浑圆状、港湾状,波状消光,边部见窄的溶蚀反应带;基质含量约82%,多为不规则潜晶状石英基晶包含针状斜长石客晶,少量石英呈他形粒状,内包含斜长石微晶,局部见少数小球粒分布,球粒界限清楚,由放射状长英质纤维组成。

2 分析方法

本文主要对特克斯达坂一带双峰式火山岩进行了LA-ICP-MS锆石U-Pb定年、主量元素与微量元素分析、Sr-Nd同位素测试以及锆石原位微区Hf同位素测试,分析方法如下:

锆石的激光剥蚀电感耦合等离子体质谱(LA-ICP-MS)原位U-Pb定年在西北大学大陆动力学国家重点实验室完成,采用的ICP-MS为美国Agilent公司生产的Agilent7500a,激光剥蚀系统为德国M-icro-Las公司生产的GeoLas200M,激光剥蚀束斑直径约为30 μm,激光剥蚀样品的深度为20~40 μm。锆石年龄采用标准锆石91500作为外部标准物质。选择²⁹Si作为内标,采用Glitter(ver4.0, Macquarie University)对锆石的同位素比值及元素含量进行计算,最终的年龄计算及谐和图采用Isoplot(ver3.0)完成,详细的实验原理和流程及仪器参数参见柳小明等(2002)和Yuan等(2008)。

本文采集的15件双峰式火山岩样品的主、微量

分析在长安大学成矿作用及其动力学实验室完成。主量元素采用X射线荧光光谱法(XRF),微量元素和稀土元素用电感耦合等离子体质谱法(ICP-MS)分析,分析方法详见Liang等(2000),分析精度优于5%,质量合乎要求。

Sr-Nd同位素测试在北京核工业地质研究所完成,由Triton热电离质谱仪(TIMS)测定,Sr/Nd的全流程空白分别为 20×10^{-12} 和 10×10^{-12} ,对样品的影响可以忽略。测试时 $^{143}\text{Nd}/^{144}\text{Nd}$ 值校准到 $^{146}\text{Nd}/^{144}\text{Nd} = 0.721\ 906$ 和 $^{145}\text{Nd}/^{144}\text{Nd} = 0.348\ 440$, $^{87}\text{Sr}/^{86}\text{Sr}$ 值校准到 $^{86}\text{Sr}/^{88}\text{Sr} = 0.119\ 40$ 。该仪器测量JMC Nd标样的 $^{143}\text{Nd}/^{144}\text{Nd} = 0.511\ 132 \pm 5$,测量NBS 987标准的 $^{87}\text{Sr}/^{86}\text{Sr} = 0.7102\ 53 \pm 6$,国际标准岩石样BCR-2的结果是 $^{143}\text{Nd}/^{144}\text{Nd} = 0.512\ 632 \pm 5$ 。

锆石原位微区Hf同位素测试是在西安地质调查中心自然资源部岩浆作用成矿与找矿重点实验室利用Neptune型多接收等离子体质谱仪和Geolas Pro型激光剥蚀系统联用的方法完成的,详细测试流程可参照侯可军等(2007)和Meng等(2014)。所有测试位置与U-Pb定年点位相同或靠近。每分析10个样品测点分析一次锆石标准GJ-1作为监控,本次实验GJ-1的测试精准度为0.282 030 ± 40(2SE)。

3 双峰式火山岩地质时代

于剖面第24层浅肉红色流纹岩中挑选出的单颗粒锆石为浅黄色-无色透明,自形-半自形柱状,晶体长0.1~0.2 mm,宽0.05~0.1 mm(图4),发育韵律环带和明暗相间的条带,²³²Th的含量为70.91 ×

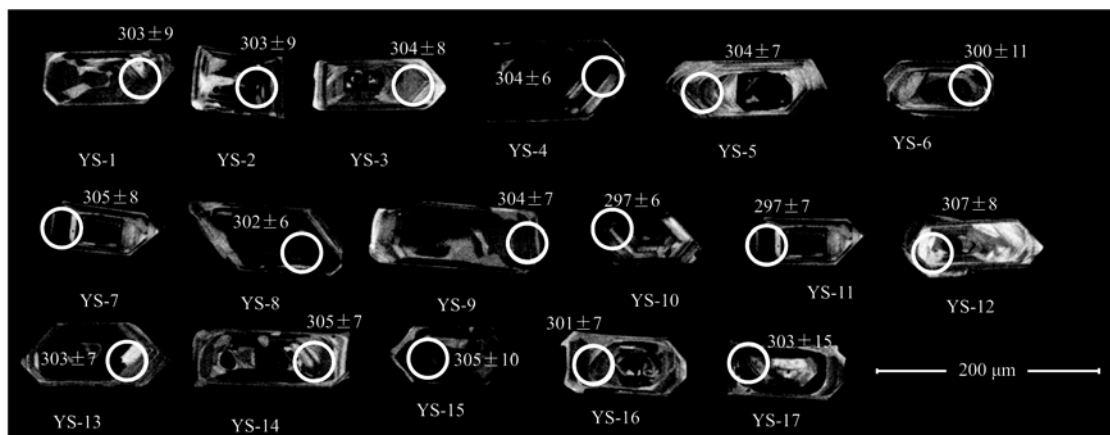


图4 伊什基里克组流纹岩样品锆石CL图像
Fig. 4 Zircon CL images of rhyolite from Yishijilike Formation

表1 伊宁地块伊什基里克组流纹岩 LA-ICP-MS 锆石 U-Pb 同位素分析结果

Table 1 LA-ICP-MS zircon U-Pb isotopic analyses of rhyolite from Yishijilike Formation of Yining landmass

点号	同位素比值										年龄/Ma				$w_B/10^{-6}$				
	$^{207}\text{Pb}/^{206}\text{Pb}$	1σ	$^{207}\text{Pb}/^{235}\text{U}$	1σ	$^{206}\text{Pb}/^{238}\text{U}$	1σ	$^{208}\text{Pb}/^{232}\text{Th}$	1σ	$^{207}\text{Pb}/^{206}\text{Pb}$	1σ	$^{207}\text{Pb}/^{235}\text{U}$	1σ	$^{206}\text{Pb}/^{238}\text{U}$	1σ	$^{208}\text{Pb}/^{232}\text{Th}$	1σ			
YS-1	0.05270	0.00583	0.34910	0.03788	0.04811	0.00141	0.01468	0.00086	316	191	304	29	303	9	295	17	142.09	274.25	0.518
YS-2	0.05227	0.00576	0.35304	0.03818	0.04904	0.00140	0.01611	0.00087	297	191	307	29	309	9	323	17	126.62	240.98	0.525
YS-3	0.05238	0.00488	0.34817	0.03186	0.04827	0.00123	0.01398	0.00074	302	161	303	24	304	8	281	15	70.91	172.66	0.411
YS-4	0.05276	0.00276	0.35131	0.01791	0.04834	0.00100	0.01462	0.00042	318	78	306	13	304	6	293	8	160.00	311.58	0.514
YS-5	0.05241	0.00367	0.34852	0.02383	0.04827	0.00110	0.01533	0.00054	303	114	304	18	304	7	308	11	161.41	299.40	0.539
YS-6	0.05268	0.00855	0.34617	0.05526	0.04769	0.00171	0.01487	0.00131	315	290	302	42	300	11	298	26	86.43	187.16	0.462
YS-7	0.05267	0.00561	0.35175	0.03676	0.04845	0.00134	0.01594	0.00084	315	185	306	28	305	8	320	17	108.65	223.51	0.486
YS-8	0.05265	0.00302	0.34757	0.01940	0.04789	0.00099	0.01475	0.00044	314	89	303	15	302	6	296	9	166.25	322.17	0.516
YS-9	0.05254	0.00399	0.34916	0.02599	0.04821	0.00110	0.01456	0.00059	309	128	304	20	304	7	292	12	114.28	248.51	0.460
YS-10	0.05226	0.00370	0.34023	0.02353	0.04722	0.00105	0.01408	0.00051	297	117	297	18	297	6	283	10	156.70	297.53	0.527
YS-11	0.05281	0.00464	0.34340	0.02957	0.04716	0.00116	0.01413	0.00066	321	151	300	22	297	7	284	13	122.80	243.03	0.505
YS-12	0.05262	0.00530	0.35387	0.03495	0.04877	0.00128	0.01612	0.00079	312	175	308	26	307	8	323	16	93.19	188.21	0.495
YS-13	0.05305	0.00481	0.35167	0.03132	0.04806	0.00115	0.01449	0.00068	331	158	306	24	303	7	291	14	82.41	182.59	0.451
YS-14	0.05225	0.00385	0.34962	0.02510	0.04851	0.00111	0.01460	0.00053	296	122	304	19	305	7	293	11	187.71	319.27	0.588
YS-15	0.05215	0.00769	0.34891	0.05052	0.04847	0.00166	0.01340	0.00118	292	260	304	38	305	10	269	24	88.05	197.20	0.447
YS-16	0.05289	0.00499	0.34843	0.03223	0.04772	0.00116	0.01281	0.00067	324	165	304	24	301	7	257	13	85.20	191.05	0.446
YS-17	0.05243	0.01168	0.34856	0.07608	0.04814	0.00245	0.01607	0.00199	304	354	304	57	303	15	322	40	104.17	229.89	0.453

$10^{-6} \sim 187.71 \times 10^{-6}$, ^{238}U 的含量为 $172.66 \times 10^{-6} \sim 311.58 \times 10^{-6}$, Th、U 含量呈现出较好的正相关关系, 有较高的 Th/U 值 ($0.411 \sim 0.588$) (表 1), 具有典型岩浆成因的锆石特征 (Williams *et al.*, 1996; Claesson *et al.*, 2000; Hoskin and Black, 2000)。所

有锆石数据点均落在谐和线上及附近 (图 5), $^{206}\text{Pb}/^{238}\text{U}$ 加权平均年龄为 302.8 ± 3.6 Ma (MSWD = 0.18, $n = 17$, 95% 置信度), 时代为晚石炭世, 代表双峰式火山岩的成岩年龄。

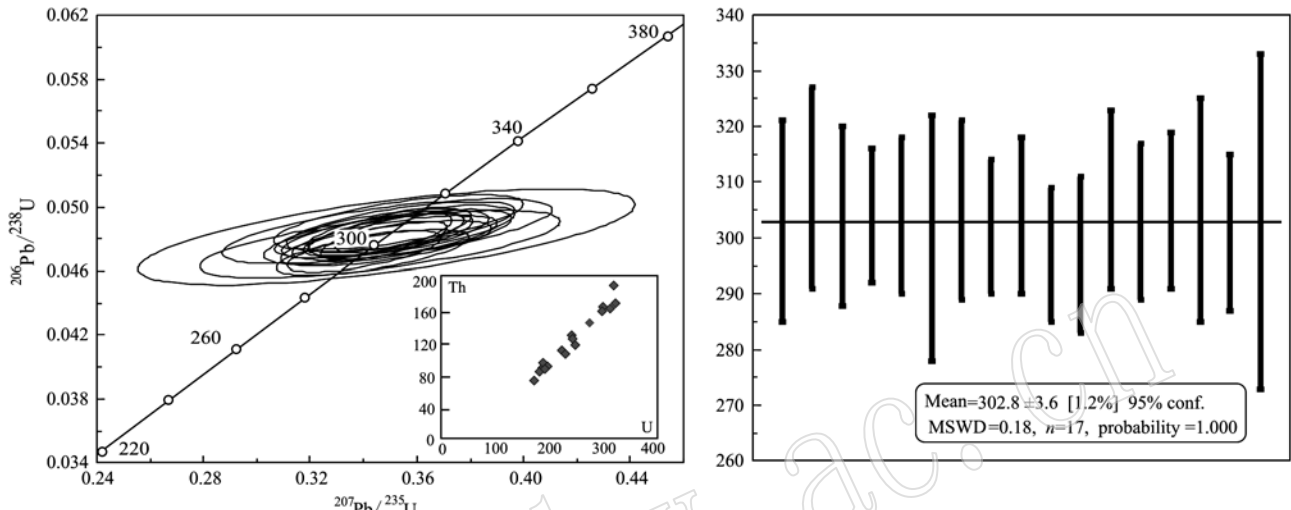


图 5 伊什基里克组锆石 U-Pb 年龄谐和图

Fig. 5 Zircon U-Pb concordia diagram of rhyolite from Yishijilike Formation

4 双峰式火山岩地球化学特征

4.1 主量元素地球化学特征

样品来自实测剖面的第 18、24 层 (图 2), 相关数据见表 2。双峰式火山岩中的玄武岩/玄武安山岩样品具有低 SiO_2 ($47.13\% \sim 53.62\%$)、高 Fe_2O_3 ($\text{TiFe}_2\text{O}_3 = 10.90\% \sim 17.40\%$)、 MgO ($3.74\% \sim 10.12\%$, 平均为 6.48%) 和高 Na ($\text{Na}_2\text{O} = 2.84\% \sim 6.69\%$)、低 K ($\text{K}_2\text{O} = 0.48\% \sim 3.77\%$) 特征 ($\text{Na}_2\text{O}/\text{K}_2\text{O} = 1.21 \sim 12.18$), $\text{Mg}^{\#}$ 值较小 ($34.36 \sim 59.83$, 平均为 46.70)。主量元素含量变化范围较大, 这可能与岩浆上涌过程的地壳同化混染作用 (AFC) 有关。在 TAS(图 6a) 图解中, 玄武岩样品落入了碱性岩浆系列, 与高的里特曼指数 (δ) $3.28 \sim 9.07$ 相对应。

与玄武岩/玄武安山岩相比, 流纹岩样品具有高 SiO_2 ($72.15\% \sim 77.72\%$)、高 K ($\text{K}_2\text{O} = 6.12\% \sim 9.48\%$)、低 Na ($\text{Na}_2\text{O} = 0.40\% \sim 2.39\%$) 特征 ($\text{Na}_2\text{O}/\text{K}_2\text{O} = 0.04 \sim 0.36$), $\text{Mg}^{\#}$ 值较小 ($2.17 \sim 22.62$, 平均为 13.59), 且其他氧化物含量较为集中 (Al_2O_3 、 P_2O_5 、 TiO_2 等)。在 TAS 图解 (图 6a) 中, 样品同样落入了碱性岩浆系列, 通过计算分析得到源区流纹岩的碱度率 (AR) 在 $4.08 \sim 11.20$ 之间, 基本

属于碱性系列。在 TAS(图 6a) 和 $\text{Zr}/\text{Ti} - \text{Nb}/\text{Y}$ (图 6b) 图解中, 酸性岩浆与基性岩浆之间存在明显的两群性, SiO_2 含量在 $53.62\% \sim 72.15\%$ 区间出现缺失, 为典型的双峰式火山岩特征。

4.2 微量元素地球化学特征

玄武岩稀土元素总量相对较低 ($\sum \text{REE} = 82.32 \times 10^{-6} \sim 240.97 \times 10^{-6}$, 平均为 160.47×10^{-6}), 轻重稀土元素分异明显, $(\text{La}/\text{Yb})_{\text{N}} = 1.58 \sim 4.94$, 轻稀土元素与重稀土元素内部分馏较弱 (图 7)。在球粒陨石标准化图中表现为 V 字型分布, 具有 δEu 负异常特征 ($\delta\text{Eu} = 0.30 \sim 1.10$); 在原始地幔标准化图解中, 大离子亲石元素 (LILE) 略有富集, 亏损 Ta 、 Nb 、 Th 、 Sr 等不相容元素 (图 8), 与洋脊玄武岩 (MORB)、洋岛玄武岩 (OIB) 明显不同 (Sun and McDonough, 1989)。

流纹岩稀土元素总量总体高于玄武岩稀土元素总量 ($\sum \text{REE} = 88.22 \times 10^{-6} \sim 424.55 \times 10^{-6}$, 平均为 194.64×10^{-6}), 轻重稀土元素分异明显, $(\text{La}/\text{Yb})_{\text{N}} = 2.46 \sim 10.48$ (图 7)。在球粒陨石标准化图解中, 流纹岩和玄武岩均具有明显的 V 字型分布和 δEu 负异常特征 (流纹岩的 δEu 值为 $0.18 \sim 0.44$); 在原始地幔标准化图解中, 流纹岩 K 、 Rb (LILE) 和 LREE 显著富集, 相对亏损 Ba 、 Sr 、 P 、 Ti (图 8)。

表2 伊什基里克组火山岩主量元素($w_B/\%$)、微量元素($w_B/10^{-6}$)分析结果Table 2 The concentrations of major ($w_B/\%$) and trace elements ($w_B/10^{-6}$) of volcanic rocks from Yishijilike Formation

岩性 样号	流纹岩								
	SF1-1	SF1-3	SF1-5	SF1-7	SF1-9	SF1-11	SF2-1	SF2-5	SF2-7
SiO ₂	75.59	74.75	74.47	74.73	75.26	75.59	76.77	77.72	76.17
TiO ₂	0.20	0.19	0.19	0.21	0.18	0.23	0.20	0.18	0.19
Al ₂ O ₃	12.09	12.14	11.88	12.69	11.62	11.77	12.29	11.47	11.94
TFe ₂ O ₃	2.51	2.63	3.03	1.98	3.35	3.17	1.16	1.41	2.23
MnO	0.02	0.04	0.04	0.01	0.04	0.04	0.00	0.01	0.02
MgO	0.30	0.36	0.45	0.21	0.36	0.46	0.09	0.01	0.08
CaO	0.22	0.20	0.96	0.51	0.22	0.99	0.17	0.14	0.38
Na ₂ O	2.23	1.13	1.97	2.02	1.50	1.61	1.52	1.63	2.39
K ₂ O	6.82	8.53	7.00	7.60	7.47	6.12	7.79	7.39	6.57
P ₂ O ₅	0.01	0.01	0.01	0.03	0.01	0.01	0.01	0.03	0.03
LOI	0.84	0.73	1.38	0.89	0.85	2.77	0.67	0.43	0.62
TOTAL	99.28	99.41	99.86	99.21	98.22	100.10	98.91	98.61	99.11
Na ₂ O/K ₂ O	0.33	0.13	0.28	0.27	0.20	0.26	0.19	0.36	0.09
Mg [#]	19.39	21.52	22.62	17.58	17.53	22.38	13.52	6.72	4.59
AR	6.55	8.23	5.62	6.38	7.26	4.08	6.90	6.33	9.74
Li	9.43	11.07	13.52	7.85	16.77	28.04	6.80	3.22	6.55
Be	4.58	3.69	2.81	3.98	3.39	3.65	2.46	2.07	3.30
Sc	3.52	3.98	3.87	0.77	4.06	5.23	2.40	1.36	2.18
V	6.81	7.21	14.87	7.62	10.09	7.50	4.14	4.63	9.54
Cr	0.40	0.41	0.84	3.73	0.36	2.56	0.27	0.76	0.76
Co	0.83	1.39	1.67	0.84	1.26	1.04	0.66	0.22	0.65
Ni	0.47	0.55	4.42	0.89	0.97	1.64	0.55	0.50	0.80
Cu	2.05	12.15	5.64	10.03	11.03	6.48	71.96	16.34	20.35
Zn	12.53	17.27	28.11	7.14	37.27	19.57	4.61	1.66	5.87
Ga	38.65	43.45	39.92	35.05	41.87	35.40	40.66	28.21	36.16
Rb	217.80	259.50	218.54	220.67	248.93	177.63	250.92	195.36	167.51
Sr	61.63	45.05	53.54	42.91	53.09	71.89	36.66	22.10	42.63
Y	64.26	41.40	30.36	21.04	38.62	90.50	17.24	6.16	30.29
Zr	328.24	337.55	329.32	366.58	316.45	357.71	347.72	322.60	307.03
Nb	21.53	21.54	21.72	23.27	21.48	25.34	23.30	21.05	20.63
Mo	0.83	2.36	2.37	0.58	3.28	1.24	1.23	1.15	2.40
Cd	0.43	0.40	0.42	0.46	0.56	0.65	0.40	0.35	0.34
Ba	448.16	506.33	470.85	399.96	488.80	356.73	506.86	321.47	435.02
La	36.91	38.97	33.68	16.80	40.57	81.48	25.14	4.70	26.60
Ce	80.23	84.83	62.96	34.38	87.12	173.33	56.47	22.90	61.65
Pr	10.08	9.99	7.57	4.55	10.60	19.84	5.85	1.16	7.20
Nd	41.11	39.94	28.21	18.79	39.58	73.54	21.62	4.49	29.17
Sm	9.85	8.64	5.77	4.12	7.78	14.46	4.12	0.96	6.36
Eu	0.73	0.67	0.53	0.41	0.65	0.91	0.46	0.18	0.56
Gd	10.73	8.39	5.34	4.34	7.35	15.34	4.04	1.10	6.34
Tb	1.86	1.30	0.91	0.75	1.20	2.54	0.64	0.17	1.03
Dy	12.00	8.18	6.10	4.76	7.76	16.20	4.12	1.14	6.43
Ho	2.73	1.90	1.44	1.10	1.85	3.78	0.96	0.28	1.45
Er	7.37	5.38	4.28	3.03	5.39	10.30	2.72	0.86	4.05
Tm	1.14	0.89	0.74	0.49	0.93	1.56	0.42	0.14	0.64
Yb	7.23	5.93	5.25	3.11	6.40	9.79	2.78	0.98	4.08
Lu	1.09	0.93	0.81	0.50	1.01	1.48	0.43	0.16	0.63
Hf	10.13	10.62	10.01	11.00	9.88	11.18	10.90	9.68	9.21
Ta	1.50	1.50	1.46	1.40	1.48	1.72	1.56	1.41	1.39
Pb	2.81	8.08	16.63	8.71	69.87	4.73	24.37	2.31	2.34
Bi	0.21	0.10	0.05	0.76	0.28	0.16	0.23	0.27	0.35
Th	22.32	22.58	21.00	10.10	21.53	24.56	20.68	8.33	15.68
U	7.57	6.65	8.59	4.57	9.49	6.74	5.67	3.91	4.62
K	28 287.79	35 410.42	29 034.83	31 530.21	30 985.42	25 412.51	32 316.27	30 687.51	27 262.16
P	22.16	22.10	22.15	66.55	22.40	22.41	22.20	66.64	66.43
Ti	1 218.00	1 154.29	1 156.63	1 280.46	1 108.25	1 355.08	1 220.48	1 099.10	1 156.51
ΣREE	223.05	215.93	163.59	97.12	218.19	424.55	129.78	39.24	156.19
(La/Yb) _N	3.66	4.71	4.60	3.88	4.55	5.97	6.48	3.45	4.68
δEu	0.22	0.24	0.29	0.30	0.26	0.18	0.34	0.27	0.25

续表 2-1

Continued Table 2-1

岩性 样号	流纹岩					玄武岩			
	SF2-9	SF2-11	SF2-13	SF2-15	SF2-19	SF1-4	SF1-6	SF1-8	SF1-10
SiO ₂	76.95	75.35	75.73	72.15	77.56	51.79	51.34	47.29	48.53
TiO ₂	0.17	0.18	0.19	0.21	0.17	2.04	1.67	2.26	1.77
Al ₂ O ₃	11.10	11.64	12.21	13.33	10.66	16.04	16.20	19.20	15.87
TFe ₂ O ₃	2.34	2.72	1.22	3.01	2.53	12.95	14.10	13.46	13.99
MnO	0.01	0.01	0.02	0.05	0.01	0.43	0.34	0.47	0.33
MgO	0.12	0.03	0.04	0.19	0.23	6.82	7.60	10.12	9.06
CaO	0.37	0.17	0.88	0.38	0.20	3.44	2.33	3.21	4.65
Na ₂ O	1.20	0.40	1.74	1.51	0.87	5.81	5.64	2.84	4.47
K ₂ O	7.74	9.48	7.95	9.14	7.75	0.48	0.62	0.91	1.20
P ₂ O ₅	0.01	0.01	0.01	0.02	0.02	0.20	0.17	0.25	0.14
LOI	0.61	0.51	0.97	0.80	0.58	5.16	5.73	10.73	4.56
TOTAL	99.09	99.10	99.09	99.20	99.93	99.50	99.58	100.12	99.60
Na ₂ O/K ₂ O	0.15	0.04	0.22	0.17	0.11	12.18	9.12	3.14	3.73
Mg [#]	9.36	2.17	6.19	11.28	15.36	51.03	51.62	59.83	56.18
AR(δ)	8.07	11.20	6.71	7.96	8.68	4.49	4.69	3.28	5.82
Li	6.72	4.47	5.21	0.85	6.10	50.99	60.77	100.30	103.29
Be	3.05	3.16	3.55	4.73	2.59	2.72	2.89	4.26	0.74
Sc	2.49	2.54	2.02	3.26	2.88	43.81	31.91	31.17	32.32
V	4.88	3.48	6.07	21.16	2.39	309.14	241.66	217.80	252.14
Cr	0.47	0.51	0.59	2.41	0.30	161.36	140.78	29.48	194.57
Co	0.85	0.44	0.46	4.95	0.80	35.96	34.72	47.16	49.16
Ni	0.57	0.55	0.87	2.70	0.58	47.29	86.60	95.55	137.47
Cu	23.56	11.35	23.65	55.56	9.25	114.05	78.85	108.76	14.47
Zn	6.03	5.46	3.68	6.40	7.45	239.83	243.81	1087.15	199.67
Ga	39.40	35.55	43.00	45.04	37.15	30.06	25.17	35.42	48.97
Rb	202.30	249.26	199.52	220.33	208.13	35.68	42.40	60.87	50.75
Sr	28.09	17.55	37.49	39.98	20.80	226.73	217.70	207.09	541.20
Y	22.68	29.42	22.65	43.25	48.25	90.93	91.18	92.47	28.22
Zr	310.83	334.06	330.15	323.90	290.96	139.56	122.09	126.66	100.27
Nb	20.07	21.08	20.03	20.16	19.69	4.09	4.77	3.00	3.47
Mo	0.76	1.36	0.47	0.74	0.83	0.58	1.59	0.89	0.39
Cd	0.33	0.37	0.36	0.36	0.31	0.57	0.26	0.54	0.29
Ba	483.84	427.55	556.60	571.10	436.32	78.57	99.07	66.24	615.87
La	17.91	52.14	12.66	38.39	32.50	21.58	32.34	21.50	11.45
Ce	41.77	130.32	34.92	106.79	84.85	47.10	71.30	43.64	24.83
Pr	4.76	14.46	3.52	10.62	9.03	7.07	10.19	8.39	3.50
Nd	19.87	57.57	14.66	42.89	34.70	34.71	46.10	42.24	16.88
Sm	4.53	11.02	3.55	10.16	7.40	9.30	12.95	11.00	4.47
Eu	0.59	0.62	0.54	0.97	0.60	1.89	1.40	2.06	1.76
Gd	4.46	9.92	3.89	10.45	7.71	13.21	15.78	14.56	5.37
Tb	0.70	1.28	0.69	1.64	1.31	2.08	2.67	2.20	0.84
Dy	4.32	6.78	4.63	9.39	8.62	12.92	15.99	13.27	5.21
Ho	1.01	1.43	1.11	1.99	2.06	3.07	3.44	3.17	1.19
Er	2.81	3.74	3.26	5.31	5.79	7.65	8.13	7.86	3.10
Tm	0.45	0.56	0.54	0.83	0.94	0.97	1.05	1.01	0.45
Yb	3.01	3.57	3.69	5.39	6.19	5.28	5.63	5.53	2.84
Lu	0.48	0.54	0.56	0.81	0.97	0.82	0.81	0.84	0.43
Hf	9.31	10.07	9.86	9.82	8.84	3.62	3.34	3.30	2.73
Ta	1.36	1.42	1.40	1.43	1.33	0.26	0.32	0.22	0.23
Pb	13.05	4.44	4.13	21.08	13.84	58.48	32.53	167.67	27.30
Bi	0.12	0.04	0.16	0.50	0.25	0.03	0.23	0.01	0.05
Th	15.18	22.00	14.37	19.26	18.48	0.70	2.32	0.35	0.61
U	3.95	7.20	3.97	4.25	4.47	1.88	3.82	4.39	0.46
K	32 111.09	39 357.44	32 990.22	37 915.14	32 164.07	1 979.54	2 564.73	3 760.49	4 977.90
P	22.15	22.12	22.23	44.33	43.91	439.25	371.83	536.77	298.33
Ti	1 034.88	1 094.53	1 160.87	1 279.42	1 025.82	12 200.98	10 028.93	13 547.26	10 597.22
ΣREE	106.66	293.95	88.22	245.62	202.66	167.63	227.78	177.29	82.32
(La/Yb) _N	4.27	10.48	2.46	5.11	3.77	2.93	4.12	2.79	2.89
δEu	0.40	0.18	0.44	0.29	0.24	0.52	0.30	0.50	1.10

续表 2-2
Continued Table 2-2

岩性 样号	玄武岩								
	SF2-2	SF2-4	SF2-6	SF2-8	SF2-10	SF2-12	SF2-14	SF2-16	SF2-18
SiO ₂	47.13	52.49	50.88	50.23	50.04	51.57	53.62	53.35	48.97
TiO ₂	3.51	2.03	2.76	2.51	2.77	1.99	2.15	2.88	3.15
Al ₂ O ₃	13.19	16.62	14.26	14.72	15.94	15.80	16.25	13.62	14.92
TFe ₂ O ₃	17.40	12.12	15.68	17.12	13.37	13.43	10.90	14.14	17.30
MnO	0.98	0.48	0.82	0.31	0.63	0.70	0.83	0.76	0.58
MgO	5.28	6.58	5.15	5.34	4.15	7.34	6.83	3.74	6.26
CaO	6.36	1.12	2.99	2.27	6.65	1.95	1.36	3.60	1.09
Na ₂ O	4.34	4.60	5.56	5.41	4.51	5.72	6.69	5.00	4.02
K ₂ O	1.25	3.77	1.73	1.91	1.24	1.31	1.10	2.04	3.34
P ₂ O ₅	0.54	0.19	0.17	0.19	0.70	0.19	0.26	0.86	0.37
LOI	4.56	2.78	4.71	3.46	4.26	2.72	4.61	5.29	2.61
TOTAL	99.25	99.23	99.52	98.03	98.43	98.07	98.80	99.98	100.37
Na ₂ O/K ₂ O	3.46	1.22	3.22	2.83	3.63	4.39	6.08	2.45	1.21
Mg [#]	37.51	51.80	39.42	38.20	38.05	51.98	55.39	34.36	41.74
δ	7.58	7.38	6.73	7.40	4.71	5.76	5.72	4.79	9.07
Li	37.77	53.83	20.88	23.52	19.59	47.11	36.62	17.32	38.11
Be	1.44	1.61	1.66	3.01	2.03	1.05	1.73	2.59	1.32
Sc	59.26	33.41	45.81	47.75	35.62	40.26	40.33	31.68	41.59
V	431.04	274.90	364.06	367.65	233.33	298.85	286.36	170.44	350.89
Cr	95.04	137.39	18.91	15.12	16.92	111.57	158.70	13.56	13.24
Co	45.54	39.28	40.80	48.46	25.79	36.69	36.46	24.78	40.12
Ni	27.17	29.57	18.31	16.32	12.84	40.71	28.23	7.94	16.67
Cu	171.59	66.79	155.85	145.37	164.37	66.75	136.67	150.64	138.39
Zn	128.11	189.23	159.47	155.62	93.89	171.99	183.28	86.53	267.58
Ga	35.55	135.82	34.73	39.37	37.56	30.41	35.18	34.77	43.39
Rb	51.94	67.02	43.03	50.97	39.78	46.84	29.20	39.47	45.02
Sr	432.28	213.03	178.65	150.80	328.26	218.62	172.45	232.56	112.15
Y	53.42	51.83	50.68	56.94	58.06	33.39	55.53	81.02	60.86
Zr	236.21	152.37	182.03	167.55	281.28	121.67	145.92	368.46	207.90
Nb	6.75	12.80	6.30	5.66	9.58	4.08	5.59	15.51	7.39
Mo	1.04	0.98	0.86	1.38	0.80	0.96	0.97	0.90	1.11
Cd	0.29	0.16	0.21	0.19	0.35	0.14	0.16	0.56	0.22
Ba	269.63	1916.45	217.25	234.21	257.37	170.26	161.50	207.69	284.37
La	12.84	16.58	19.87	32.31	19.72	14.79	19.96	29.77	27.85
Ce	37.75	36.65	45.56	65.36	53.08	32.95	45.09	75.38	57.59
Pr	5.88	5.20	6.23	8.13	7.79	4.50	6.71	10.99	8.04
Nd	29.76	24.51	29.16	36.27	37.36	21.38	32.64	51.57	36.52
Sm	8.41	6.63	7.43	8.26	9.70	5.02	9.00	13.38	8.82
Eu	2.67	2.00	2.23	2.09	2.92	1.58	1.36	3.34	2.02
Gd	9.65	8.40	8.64	10.02	10.72	5.91	10.42	14.91	10.46
Tb	1.62	1.35	1.40	1.53	1.75	0.91	1.64	2.44	1.65
Dy	10.39	8.64	8.78	9.44	10.95	5.72	9.89	15.24	10.20
Ho	2.35	1.99	2.02	2.12	2.46	1.32	2.22	3.48	2.31
Er	6.18	5.20	5.24	5.43	6.43	3.50	5.79	9.21	5.98
Tm	0.92	0.75	0.76	0.77	0.96	0.51	0.83	1.37	0.86
Yb	5.83	4.51	4.71	4.69	6.03	3.18	4.96	8.59	5.23
Lu	0.87	0.68	0.70	0.70	0.91	0.49	0.73	1.31	0.80
Hf	6.03	3.91	4.79	4.45	6.96	3.26	3.78	10.41	5.47
Ta	0.40	1.55	0.37	0.33	0.54	0.25	0.31	0.93	0.42
Pb	60.81	4.68	165.14	11.86	2.24	20.78	3.25	92.55	13.25
Bi	0.13	0.19	0.06	0.11	0.03	0.12	0.33	0.03	0.09
Th	1.33	1.69	1.67	1.56	2.66	1.12	1.29	5.00	2.08
U	0.72	1.58	0.81	1.35	0.82	0.74	1.54	1.46	1.37
K	5 205.25	15 630.55	7 171.56	7 922.04	5 159.86	5 417.29	4 571.17	8 481.57	13 851.09
P	1 175.62	415.34	363.27	418.66	1 526.77	420.05	559.77	1 881.52	816.59
Ti	21 066.70	12 177.74	16 538.36	15 024.26	16 598.84	11 930.99	12 886.27	17 239.40	18 854.62
ΣREE	135.11	123.08	142.75	187.13	170.79	101.75	151.24	240.97	178.35
(La/Yb) _N	1.58	2.64	3.02	4.94	2.35	3.34	2.88	2.49	3.82
δEu	0.90	0.82	0.85	0.70	0.87	0.89	0.43	0.72	0.64

注: TFe₂O₃ 表示全铁; LOI 为烧失量; Mg[#] = Mg²⁺/(Mg²⁺ + Fe²⁺); AR = (Al₂O₃ + CaO + Na₂O + K₂O)/(Al₂O₃ + CaO - Na₂O - K₂O); δ = (Na₂O + K₂O)²/(SiO₂ - 43); (La/Yb)_N 为球粒陨石标准化比值; δEu = Eu_N/(Sm_N × Gd_N)^{1/2}; 标准化值引自 Boynton (1984)。

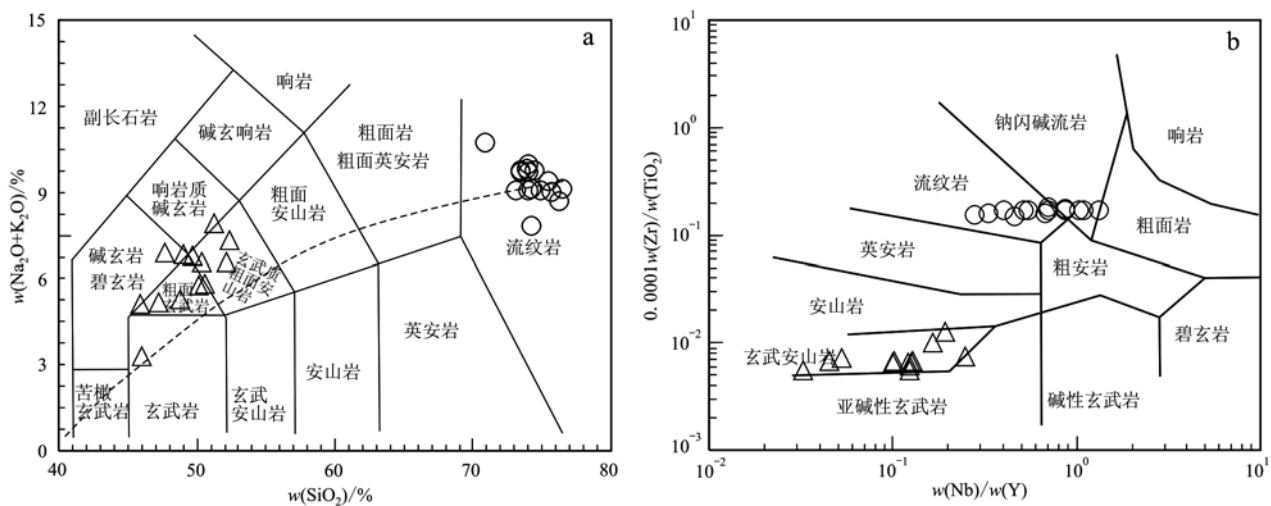


图 6 伊什基里克组火山岩 TAS(a, 据 Le et al., 1986) 和 Zr/TiO₂ – Nb/Y(b, 据 Winchester and Floyd, 1977) 图解
Fig. 6 TAS (a, after Le et al., 1986) and Zr/TiO₂ versus Nb/Y (b, after Winchester and Floyd, 1977) diagrams of volcanic rocks from Yishijilike Formation

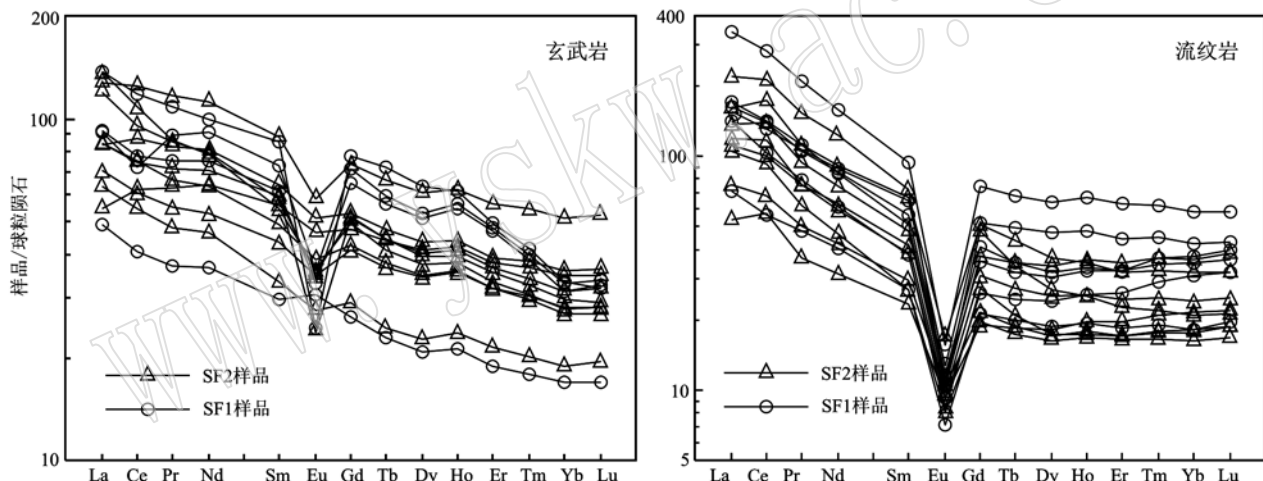


图 7 伊什基里克组火山岩球粒陨石标准化稀土元素配分图(标准值据 Boynton, 1984)
Fig. 7 Chondrite-normalized REE patterns of volcanic rocks from Yishijilike Formation (normalization values after Boynton, 1984)

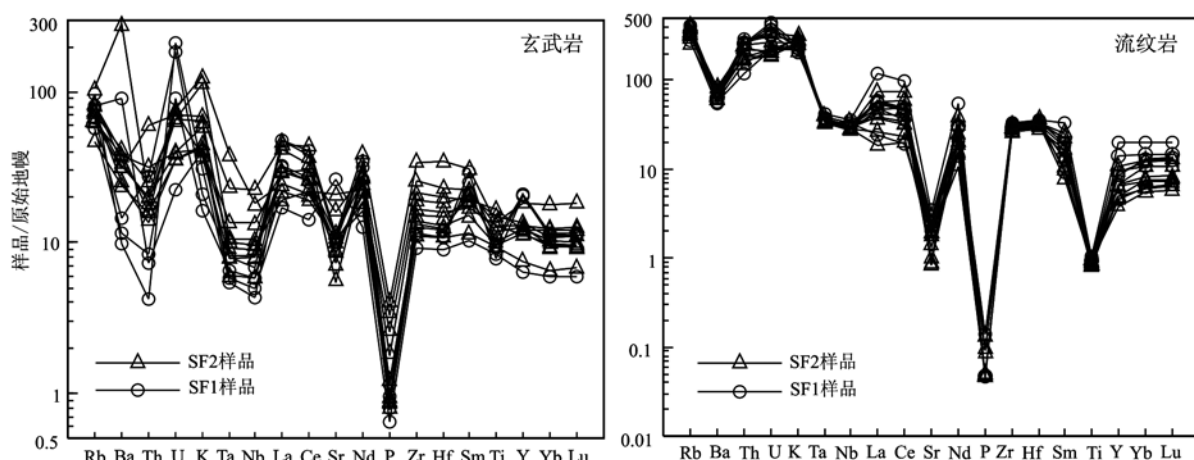


图 8 伊什基里克组火山岩原始地幔标准化微量元素蛛网图(标准值据 Sun and McDonough, 1989)
Fig. 8 Primitive mantle-normalized trace element spider diagrams of volcanic rocks from Yishijilike Formation (normalization values after Sun and McDonough, 1989)

4.3 双峰式火山岩同位素组成与变化

伊什基里克组火山岩的 Sr-Nd 同位素分析数据见表 3。按 302.8 Ma 校正获得 2 个玄武岩样品 ($^{87}\text{Sr}/^{86}\text{Sr}$)_i 值分别为 0.705 8 和 0.705 4, 对应的 $\varepsilon\text{Nd}(t)$ 值分别为 3.55 和 3.45; 而 1 个流纹岩的

($^{87}\text{Sr}/^{86}\text{Sr}$)_i 值为 0.702 3, $\varepsilon\text{Nd}(t)$ 值为 2.88(表 3), 表明玄武岩来自于亏损地幔, 而流纹岩则表现出新生下地壳部分熔融的特征, 这与新疆天山地区晚古生代大部分壳源岩石具有正的 $\varepsilon\text{Nd}(t)$ 值相一致(Zhu et al., 2009; 赵乐强, 2017)。

表 3 伊什基里克组火山岩 Sr-Nd 同位素比值特征

Table 3 LA-ICP-MS zircon Sr-Nd isotopic analyses of volcanic rocks from Yishijilike Formation

样品号	岩性	$^{87}\text{Rb}/^{86}\text{Sr}$	$^{87}\text{Sr}/^{86}\text{Sr}$	($^{87}\text{Sr}/^{86}\text{Sr}$) _i	$^{147}\text{Sm}/^{144}\text{Nd}$	$^{143}\text{Nd}/^{144}\text{Nd}$	($^{143}\text{Nd}/^{144}\text{Nd}$) _i	$\varepsilon\text{Nd}(t)$
SF2-1	流纹岩	1.381 174 3	0.708 373	0.702 3	0.154 6	0.512 700	0.512 386	2.88
SF2-2	玄武岩	0.129 972 3	0.706 320	0.705 8	0.165 3	0.512 758	0.512 431	3.55
SF2-4	玄武岩	0.112 171 9	0.705 858	0.705 4	0.163 8	0.512 758	0.512 426	3.45

流纹岩测年样品(SF2-1)的锆石原位 Lu-Hf 同位素测试数据(表 4)显示, 大多数锆石的 $^{176}\text{Lu}/^{177}\text{Hf}$ 值小于 0.002, 说明由 ^{176}Lu 衰变生成的 ^{176}Hf 极少, 所测定的 $^{176}\text{Hf}/^{177}\text{Hf}$ 值可以代表该锆石形成时的 $^{176}\text{Hf}/^{177}\text{Hf}$ 值(Knudsen et al., 2001; Kinny, 2003; 第五春荣等, 2007; 吴福元等, 2007)。年龄样品的 f_{Lu}/Hf 平均值为 -0.96, 明显小于镁铁质地壳的 f_{Lu}/Hf (-0.34; Amelin et al., 1999) 和硅铝质地壳的 f_{Lu}/Hf (-0.72; Vervoort et al., 1999) 值, 因此二阶段模式年龄更能反映其源区物质从亏损地幔被抽取的时间。 $^{176}\text{Hf}/^{177}\text{Hf} = 0.282\ 702 \sim 0.282\ 805$, $\varepsilon\text{Hf}(t)$ 值绝大部分大于 0(-1.1 ~ +8.3), 指示成岩岩浆由新生地壳形成。所有测点的一阶段模式年龄(t_{DM1})和二阶段模式年龄(t_{DM2})均大于 302.8 Ma, 说明锆石是岩浆重熔的产物。锆石 Hf 同位素指示流纹岩是壳源岩石重熔的产物, 表明伊什基里克组双峰式火山岩中流纹岩的源区可能与元古宙的变质结晶基底有关。

5 讨论

5.1 双峰式火山岩成因

目前对于双峰式火山岩的成因机制主要有两种观点: 一是流纹岩和玄武岩具有共同的幔源母岩浆, 流纹岩是经玄武质岩浆结晶分异作用形成的, 其中只有少量或没有陆壳物质的加入(Grove and Donnelly-Nolan, 1986; MacDonald, 1987)。这种来源相同的玄武岩和流纹岩一般具有相似的微量元素和 Nd 同位素特征(Brouxl et al., 1987; Hochstaedter et al., 1990; Geist et al., 1998)。另一种观点是

玄武岩和流纹岩来自不同的母岩浆, 在地幔部分熔融形成的热的基性岩浆上升过程中, 使地壳岩石发生部分熔融, 从而产生酸性岩浆。这种流纹岩的出露面积通常比玄武岩要大得多(Hildreth, 1981; Doe et al., 1982; Davies and MacDonald, 1987; Huppert and Sparks, 1988)。由于这种基性岩浆和酸性岩浆来源不同, 生成的玄武岩和流纹岩在微量元素和 Sr、Nd、Pb 同位素组成上就有很大的差异(Doe et al., 1982; Davies and MacDonald, 1987; 邱检生, 1999)。

5.1.1 玄武岩岩石成因

特克斯达坂一带伊什基里克组玄武岩样品均富集大离子亲石元素(LILE)和轻稀土元素(LREE), 亏损高场强元素(HFSE), Nb、Ta 的亏损说明火山岩可能遭受到了陆壳的混染作用或者是反映了其源区的地球化学性质。从变化不大的微量元素比值 La/Sm 值(1.53 ~ 3.91)来看, 地壳混染作用在岩浆演化过程中影响不大(可能会有微弱的混染作用), 因此其元素地球化学特征主要反映了其源区的地球化学性质(刘阁, 2014)。玄武岩样品具有相对高的 Mg[#]、Cr、Co、Ni 值, 并且其 $\varepsilon\text{Nd}(t)$ 值为 3.45、3.55, 结合 Nb-Zr 图解(图 9), 表明伊什基里克组玄武岩来源于亏损地幔。

5.1.2 流纹岩岩石成因

流纹岩具有较高的 SiO₂、K₂O + Na₂O 和极低的 TiO₂、MgO、P₂O₅、TFe₂O₃ 含量, 在稀土元素配分图上具明显的负 Eu 异常, 在微量元素标准化图上显示出 Ba、Nb、Ta、Sr、P 和 Ti 的亏损, 与 A 型花岗岩具有相似的地球化学特征(张旗等, 2012a, 2012b)。所有样品在 Zr-Ga/Al 图上均落在 A 型花岗岩区(图 10)。流纹岩具有高 SiO₂ 和极低的 MgO 含量, 表明其

表 4 伊什基里克组流纹岩的 LA-ICP-MS 锆石 Lu-Hf 同位素分析及参数计算表(样品年龄 302.8 Ma)

Table 4 LA-ICP-MS zircon Lu-Hf isotopic analyses of rhyolite from Yishijiklike Formation (the age of samples is 302.8 Ma)

点号	$^{176}\text{Yb}/^{177}\text{Hf}$	$^{176}\text{Lu}/^{177}\text{Hf}$	$^{176}\text{Hf}/^{177}\text{Hf}$	δ_{Hf}	Hf_{i}	$\varepsilon\text{Hf}(\text{t})$	t_{DM}/Ma	t_{DM2}/Ma	f_{IaHf}
SF2-1-1	0.046720	0.001586	0.282727	0.000011	0.282718	-1.6	4.7	757	1.015
SF2-1-2	0.065910	0.002212	0.282648	0.000014	0.282636	-4.4	1.8	884	1.198
SF2-1-3	0.037300	0.001280	0.282747	0.000011	0.282740	-0.9	5.5	721	964
SF2-1-4	0.043976	0.001465	0.282729	0.000011	0.282720	-1.5	4.8	752	1.009
SF2-1-5	0.082152	0.002756	0.282569	0.000013	0.282553	-7.2	-1.1	1.015	1.383
SF2-1-6	0.036694	0.001238	0.282702	0.000012	0.282695	-2.5	3.9	784	1.065
SF2-1-7	0.044118	0.001446	0.282751	0.000011	0.282743	-0.7	5.6	719	957
SF2-1-8	0.049500	0.001642	0.282759	0.000009	0.282749	-0.5	5.8	712	943
SF2-1-9	0.038058	0.001265	0.282805	0.000010	0.282797	1.2	7.5	639	835
SF2-1-10	0.040492	0.001265	0.282758	0.000010	0.282751	-0.5	5.9	705	939
SF2-1-11	0.029306	0.001013	0.282790	0.000011	0.282784	0.6	7.1	656	865
SF2-1-12	0.036462	0.001204	0.282782	0.000011	0.282775	0.4	6.7	670	885
SF2-1-13	0.026583	0.000917	0.282782	0.000012	0.282777	0.3	6.8	666	882
SF2-1-14	0.074657	0.002442	0.282721	0.000010	0.282707	-1.8	4.3	783	1.039
SF2-1-15	0.029026	0.000968	0.282798	0.000011	0.282792	0.9	7.4	644	847
SF2-1-16	0.056910	0.001878	0.282743	0.000012	0.282733	-1.0	5.2	739	981
SF2-1-17	0.045164	0.001484	0.282725	0.000010	0.282716	-1.7	4.7	757	1.017
SF2-1-18	0.044774	0.001452	0.282754	0.000010	0.282746	-0.6	5.7	715	952
SF2-1-19	0.033282	0.001122	0.282787	0.000010	0.282781	0.5	6.9	662	873
SF2-1-20	0.029856	0.001020	0.282826	0.000010	0.282820	1.9	8.3	605	784
SF2-1-21	0.030682	0.001036	0.282796	0.000011	0.282790	0.8	7.3	648	852
SF2-1-22	0.047694	0.001560	0.282735	0.000010	0.282726	-1.3	5.0	744	995
SF2-1-23	0.046519	0.001559	0.282738	0.000011	0.282729	-1.2	5.1	740	988
SF2-1-24	0.047082	0.001560	0.282771	0.000012	0.282762	-0.1	6.3	693	915
SF2-1-25	0.035518	0.001203	0.282757	0.000010	0.282751	-0.5	5.9	705	940

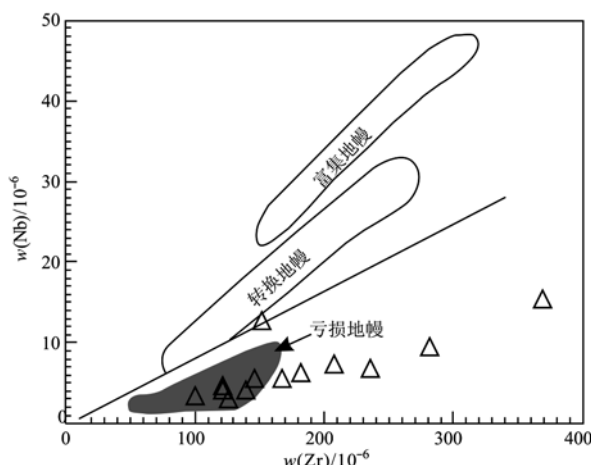


图 9 伊什基里克组玄武岩 Nb-Zr 图解

Fig. 9 Nb-Zr diagram of basalts from Yishijilike Formation

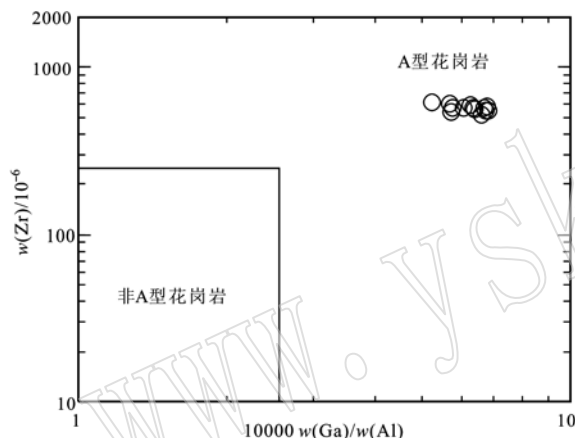
图 10 A 型花岗岩的 Zr-Ga/Al 判别图
(据 Whalen et al., 1987)

Fig. 10 Zr versus Ga/Al discrimination diagram of A-type granites (after Whalen et al., 1987)

不可能是幔源岩石直接熔融的产物;岩石具有强烈的负 Eu 异常,表明发生了斜长石的强烈分离结晶或源区有残留(刘阁, 2014);富集大离子亲石元素(LILE)和轻稀土元素(LREE),亏损 Nb、Ta 等高场强元素(HFSE),显示壳源岩浆的典型特征。伊什基里克组流纹岩的 $Rb/Sr = 2.47 \sim 14.20 (> 0.5)$, $Ti/Y = 14.97 \sim 70.79 (< 100)$ (去除 2 个异常值 178.43, 353.40), $Ti/Zr = 3.28 \sim 3.79 (< 20)$, 均位于壳源岩浆范围内(Pearce, 1983; Tischendorf and Paelchen, 1985)。同时,伊什基里克组流纹岩具有正的 $\varepsilon Hf(t)$ 值和高的 Hf 同位素比值(图 11),且在野外露头尺度体量上远大于玄武岩。这些地球化学数据与野外特征均表明伊什基里克组流纹岩与玄武岩并非是同源岩浆的产物,而是由新生玄武质下陆壳岩石部分熔融形成的。结合二阶段锆石 Hf 模式年龄,认为这种新生玄武质下地壳很可能与分布于伊宁地块内部的前寒武纪古老结晶基底有关。

5.2 双峰式火山岩产出环境

伊什基里克组双峰式火山岩的发现说明本区在晚石炭世就已经处于伸展构造阶段。不同的伸展环境所形成的火山岩具有不同的地球化学特征:大陆裂谷火山岩通常富集 LILE 和 HFSE, LREE/HREE 为明显分离的型式;而洋内岛弧火山岩中的基性岩一般为岛弧拉斑玄武岩,含有少量钙碱性和碱性系列火山岩,具有低 Ti、K, 贫 Th、Nb, 亏损 LREE、HFSE 的特征,这些与本区内火山岩的地球化学特征不一致(钱青等, 1999; 王焰等, 2000)。伊什基里克组火山岩与典型板内火山岩特征元素比值(表 5)(李

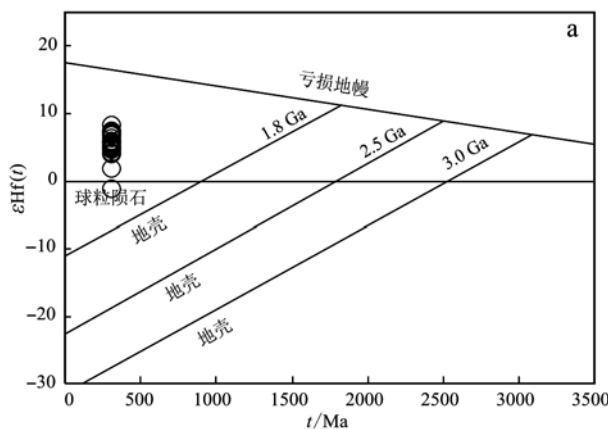
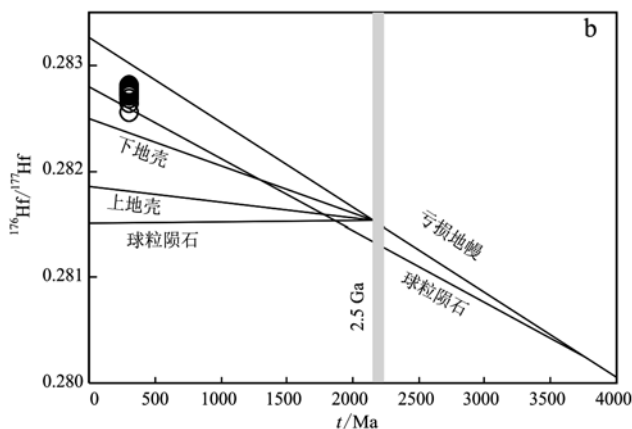


图 11 伊什基里克组流纹岩的锆石 Hf 同位素图解(吴福元等, 2007)

Fig. 11 Diagram of Hf isotope of zircon of rhyolite from Yishijilike Formation (after Wu Fuyuan et al., 2007b)



永军等, 2015) 及火山岩的构造判别图解有助于分析岩石形成的构造环境。在 $Hf/3 - Th - Ta$ 图解(图 12a)、 $Nb - Zr/4 - Y$ 图解(图 12b) 和 $FeOt - MgO - Al_2O_3$ 图解(图 12c) 中, 伊什基里克组基性岩样品均落入大陆板块内部及其附近。

A 型花岗岩可以分为 A1 型和 A2 型两个亚类(洪大卫等, 1995), 其中 A1 型花岗岩形成于板内伸

展阶段主要与地幔热柱活动有关的裂谷环境。A2 型花岗岩与板块俯冲有关的物质参与, 通常形成于后碰撞或后造山的张性构造环境(Clemens *et al.*, 1986; Whalen *et al.*, 1987; Eby, 1992)。伊什基里克组流纹岩样品在 $Nb - Y - Ga$ (图 13a) 和 $Nb - Y - Ce$ (图 13b) 图解上均落在 A2 型花岗岩区及其附近, 指示流纹岩形成于碰撞后的伸展阶段; 而在 $Y + Nb -$

表 5 伊什基里克组火山岩与典型板内火山岩特征元素比值对比表(李永军等, 2015)

Table 5 A comparison of the volcanic rocks of Yishijilike Formation with the typical intraplate volcanic rock
(after Li Yongjun *et al.*, 2015)

构造环境	大陆板内			大陆裂谷		地幔柱	本文
	大陆拉斑	大陆拉斑	大陆碱性	陆-陆碰撞	典型裂谷		
$w(Ta)/w(Hf)$	0.1~0.3	>0.3	>0.1	>0.1	>0.1	>0.3	0.08
$w(Th)/w(Ta)$	>1.6	>1.6	>10	1.64	4~10	范围大	3.98
$w(Nb)/w(Zr)$	0.04~0.15	>0.15	>0.04	>0.04	>0.04	>0.15	0.04
$w(Th)/w(Nb)$	0.11~0.67	0.11~0.67	0.11~0.67	0.11~0.27	0.27~0.67	<0.11	0.25
$w(La)/w(Nb)$	>1.1	>1.1	>2	1.1~2	1.1~2	<1.1	3.81

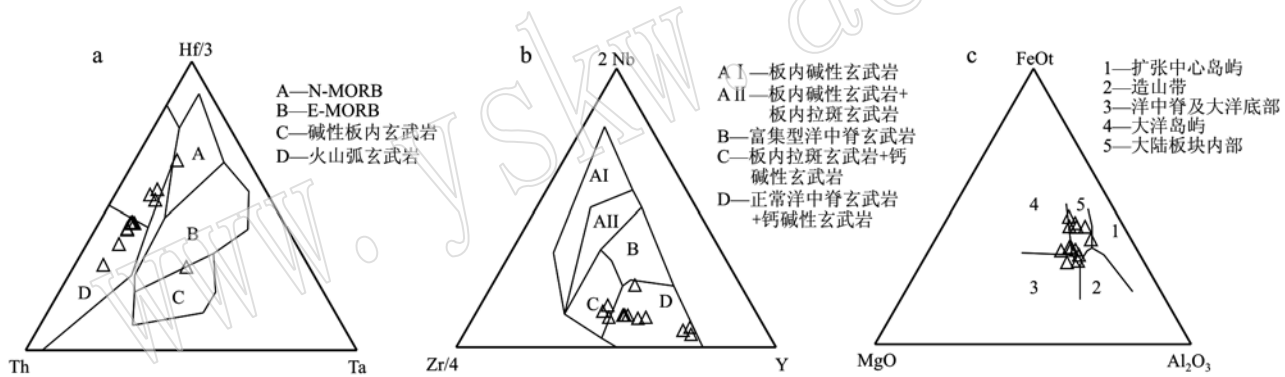


图 12 伊什基里克组玄武岩构造环境判别图解(a 据 Wood, 1980; b 据 Meschede, 1986; c 据 Pearce *et al.*, 1977)
Fig. 12 Tectonic discrimination diagrams of basalts from Yishijilike Formation (a after Wood, 1980; b after Meschede, 1986;
c, after Pearce *et al.*, 1977)

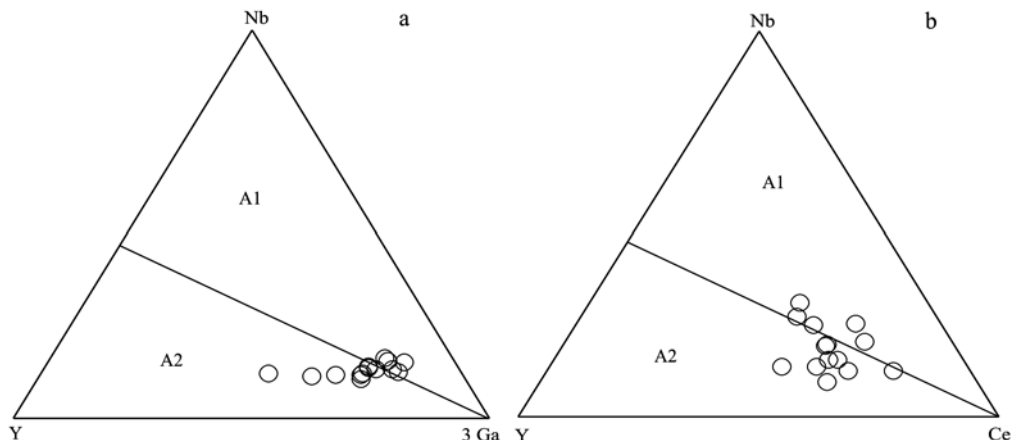
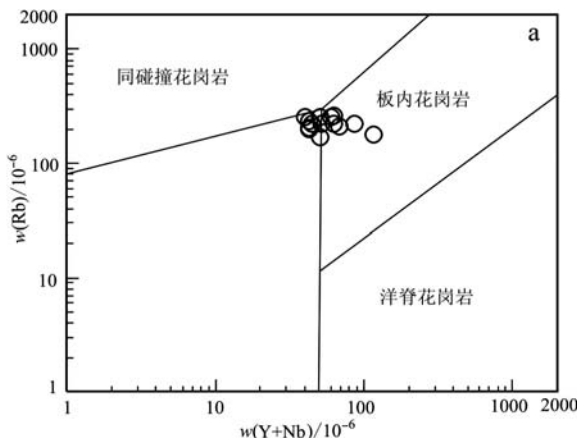


图 13 伊什基里克组流纹岩 $Nb - Y - Ga$ 图解及 $Nb - Y - Ce$ 图解(据 Eby, 1992)
Fig. 13 Diagrams of $Nb - Y - Ga$ (a) and $Nb - Y - Ce$ (b) of rhyolite from Yishijilike Formation (after Eby, 1992)

Rb(图14a)及Y-Nb(图14b)图解中,伊什基里克组流纹岩样品落入板内或碰撞后花岗岩区。

将地球化学判别图解与区内双峰式火山岩的分布、野外特征和地球化学特征综合起来,可以判断伊什基里克组双峰式火山岩形成于造山后伸展阶段,



在这一阶段,来自于亏损地幔的玄武质岩浆上涌并加热下地壳,从而产生大规模的酸性岩浆。两种截然不同的岩浆喷出最终形成伊什基里克组双峰式火山岩组合。

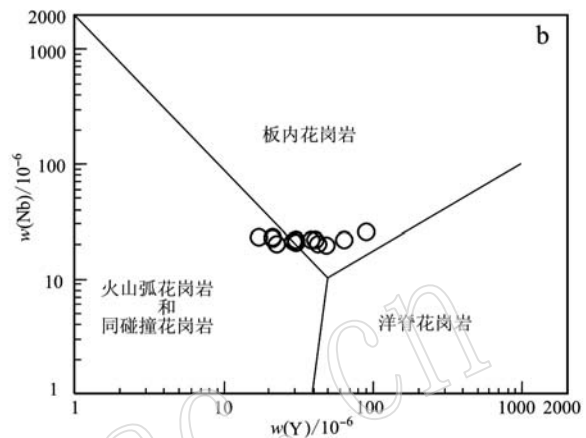


图14 伊什基里克组流纹岩Rb-Y+Nb及Nb-Y判别图(据Pearce *et al.*, 1984)

Fig. 14 Discriminant diagrams of tectonic environments of Rb versus Y + Nb (a), Nb versus Y (b) (after Pearce *et al.*, 1984)

6 结论

(1) 伊宁地块特克斯达坂一带伊什基里克组火山岩由玄武质和流纹质熔岩及少量火山碎屑岩构成,其中,玄武岩与流纹岩之间颜色对比鲜明,接触界限截然,具有双峰式火山岩特征。流纹岩出露面积或是地层厚度远远大于玄武岩,是近年来伊宁地块识别出来的最为典型的双峰式火山岩,该套双峰式火山岩年龄为 302.8 ± 3.6 Ma,形成于晚石炭世。

(2) 详细的岩石学与地球化学研究结果表明,特克斯达坂一带晚石炭世伊什基里克组双峰式火山岩形成于造山后伸展环境,具有板内成因特征。玄武岩与流纹岩来自于不同的母岩浆,玄武岩来自于亏损地幔的部分熔融,而流纹岩应是玄武质岩浆上升过程中导致地壳物质重熔而形成的,其源区可能与元古代的变质结晶基底有关。该套双峰式火山岩的发现进一步为伊宁地块石炭纪构造演化提供了重要依据。

References

Allen M B, Windley B F and Zhang C. 1993. Paleozoic collisional tectonics and magmatism of the Chinese Tien Shan, Central-Asia[J]. Tectonophysics, 220: 89 ~ 115.

Amelin Y, Lee D C, Halliday A N, *et al.* 1999. Nature of the Earth's earliest crust from hafnium isotopes in single detrital zircons[J]. Nature, 399(6733): 1497 ~ 1503.

An Fang, Zhu Yongfeng, Wei Shaoni, *et al.* 2013. An Early Devonian to Early Carboniferous volcanic arc in North Tianshan, NW China: Geochronological and geochemical evidence from volcanic rocks[J]. Journal of Asian Earth Sciences, 78: 100 ~ 113.

Boynton W V. 1984. Geochemistry of the rare earth elements: Meteorite studies[A]. Henderson P. Rare Earth Element Geochemistry[C]. Amsterdam, Netherlands: Elsevier, 63 ~ 114.

Brouxl M, Lapiere H, Michard A, *et al.* 1987. The deep layers of a Palaeozoic arc: Geochemistry of the Copley-Balaklala series, northern California[J]. Earth and Planetary Science Letters, 85(4): 386 ~ 400.

Claesson S, Vetrin V and Bayanova T. 2000. U-Pb zircon age from a Devonian carbonatite dyke, Kolapeninsula, Russia: A record of geological evolution from the Archaean to the Palaeozoic[J]. Lithos, 51(1 ~ 2): 95 ~ 108.

Clemens J D, Holloway J R and White A J R. 1986. Origin of an A-type granite: Experimental constraints[J]. American Mineralogist, 71(3 ~ 4): 317 ~ 324.

Davies G R and MacDonald R. 1987. Crustal influences in the petrogenesis of the Naivasha basalt-comendite complex: Combined trace element and Sr-Nd-Pb isotope constraints[J]. Journal of Petrology, 28(6): 1009 ~ 1031.

- Diwu Chunrong, Sun Yong, Lin Ciluan, et al. 2007. Zircon U-Pb ages and Hf isotopes and their geological significance of Yiyang TTG gneisses from Henan province, China[J]. *Acta Petrologica Sinica*, 23(2): 253~262 (in Chinese with English abstract).
- Doe B R, Leeman W P, Christlansen R L, et al. 1982. Lead and strontium isotopes and related trace elements as genetic tracers in the Upper Cenozoic rhyolite-basalt association of the Yellowstone plateau volcanic field[J]. *Journal of Geophysical Research*, 87(B6): 478~486.
- Duan Shigang, Zhang Zuoheng, Jiang Zongsheng, et al. 2014. Geology, geochemistry, and geochronology of the Dunde iron-zinc oredeposit in western Tianshan, China[J]. *Ore Geology Reviews*, 57: 441~461.
- Eby G N. 1992. Chemical subdivision of the A-type granitoids: Petrogenetic and tectonic implications[J]. *Geology*, 20(7): 641~644.
- Gao Jun, Li Maosong, Xiao Xuchang, et al. 1998. Paleozoic tectonic evolution of the Tianshan Orogen, northwestern China [J]. *Tectonophysics*, 287: 213~231.
- Gao Jun, Qian Qing, Long Lingli, et al. 2009. Accretionary orogenic process of Western Tianshan, China[J]. *Geological Bulletin of China*, 28: 1 804~1 816 (in Chinese with English abstract).
- Geist D, Howard K A and Larch P. 1998. The generation of oceanic rhyolites by crystal fractionation: The basalt-rhyolite association at Volcán Alcedo, Galápagos Archipelago[J]. *Journal of Petrology*, 36(4): 965~982.
- Ge Songsheng, Zhai Mingguo, Inna S, et al. 2015. Whole-rock geochemistry and Sr-Nd-Pb isotope systematics of the Late Carboniferous volcanic rocks of the Awulale metallogenic belt in the Western Tianshan mountains (NW China): Petrogenesis and geodynamical implications [J]. *Lithos*, 228~229: 62~77.
- Grove T L and Donnelly-Nolan J M. 1986. The evolution of young silicic clavas at Medicine Lake volcano, California: Implications for the origin of compositional gaps in calc-alkaline series lavas[J]. *Contributions to Mineralogy and Petrology*, 92(3): 281~302.
- Han Qiong, Gong Xiaoping, Ma Huadong, et al. 2015. Temporal and spatial distribution of Dahalajunshan Group volcanic rocks in the Awulale metallogenic belt of West Tianshan Mountains and its geological significance[J]. *Geology in China*, 42(3): 70~86 (in Chinese with English abstract).
- Hildreth W. 1981. Gradients in silicic magma chambers: Implications for lithospheric magmatism [J]. *Journal of Geophysical Research*, 86(B11): 10 153~10 192.
- Hochstaedter A G, Gill J B, Kusakabe M, et al. 1990. Volcanism in the Sumisu Rift I: Major element, volatile, and stable isotope geochemistry[J]. *Earth and Planetary Science Letters*, 100(1~3): 179~194.
- Hong Dawei, Wang Shi, Han Baofu, et al. 1995. Tectonic environment classification and identification sign of alkaline granite[J]. *Science in China (Series B)*, 25(4): 418~426 (in Chinese with English abstract).
- Hoskin P W O and Black L P. 2000. Metamorphic zircon formation by solidstate recrystallization of protolith igneous zircon [J]. *Journal of Metamorphic Geology*, 18: 423~439.
- Hou Kejun, Li Yanhe, Zou Tianren, et al. 2007. Laser ablation-MC-ICP-MS technique for Hf isotope microanalysis of zircon and its geological applications [J]. *Acta Petrologica Sinica*, 23(10): 2 595~2 604 (in Chinese with English abstract).
- Huppert H E and Sparks R S J. 1988. The generation of granitic magmas by intrusion of basalt into continental crust[J]. *Journal of Petrology*, 29(3): 599~624.
- Jahn B M, Wu F Y and Chen B. 2000. Granitoids of the central Asian orogenic belt and continental growth in the Phanerozoic[J]. *Transactions of the Royal Society of Edinburgh: Earth Sciences*, 91(1~2): 181~193.
- Kinny P D. 2003. Lu-Hf and Sm-Nd isotope systems in zircon[J]. *Reviews in Mineralogy and Geochemistry*, 53(1): 327~341.
- Knudsen T L, Griffin W, Hartz E, et al. 2001. In-situ hafnium and lead isotope analyses of detrital zircons from the Devonian sedimentary basin of NE Greenland: A record of repeated crustal reworking[J]. *Contributions to Mineralogy and Petrology*, 141(1): 83~94.
- Le B M J, Le M R W and Streckeisen A. 1986. A chemical classification of volcanic rocks based on the total alkali-silica diagram[J]. *Journal of Petrology*, 27: 745~750.
- Li Dapeng, Du Yangsong, Pang zhenshan, et al. 2013. Zircon U-Pb chronology and geochemistry of Carboniferous volcanic rocks in Awulale area, western Tianshan Mountains[J]. *Acta Geoscientica Sinica*, 34(2): 176~192 (in Chinese with English abstract).
- Li Jinyi, He Guoqi, Xu Xin, et al. 2006. Crustal tectonic framework of northern Xinjiang and adjacent regions and its formation[J]. *Acta Geologica Sinica*, 80(1): 148~168 (in Chinese with English abstract).
- Li Yongjun, Gao Yongli, Tong Lili, et al. 2009c. Tempestite of Ake-shake Formation in Awulale area, western Tianshan and its significance[J]. *Earth Science Frontiers*, 16(3): 341~348 (in Chinese with English abstract).
- Li Yongjun, Gu Pingyang, Pang Zhenjia, et al. 2008b. Identification of the adakite rocks of Kulesayi series and it's significance of Mo prospecting in the Tekesidaban of western Tianshan[J]. *Acta Petrologica Sinica*, 24(12): 2 713~2 719 (in Chinese with English abstract).
- Li Yongjun, Hu Keliang, Zhou Jibing, et al. 2010a. Early Carboniferous

- volcano-magma and related mineralization in the Yishijilike Mountain, western Tianshan[J]. *Earth Science—Journal of China University of Geosciences*, 35(2): 235 ~ 244 (in Chinese with English abstract).
- Li Yongjun, Jin Zhao, Hu Keliang, et al. 2010c. Discovery of fan delta-facies sediment in lower carboniferous Akeshake Formation in the Yuzan area, western Tianshan Mountains and its significance[J]. *Acta Geologica Sinica*, 84(10): 1 470 ~ 1 478 (in Chinese with English abstract).
- Li Yongjun, Li Ganyu, Tong Lili, et al. 2015. Discrimination of Ratios of Ta, Hf, Th, La, Zr and Nb for Tectonic Setting in Basalts[J]. *Journal of Earth Sciences and Environment*, 37(3): 14 ~ 21 (in Chinese with English abstract).
- Li Yongjun, Li Zhucang, Tong Lili, et al. 2010b. Revisit the constraints on the closure of the Tianshan ancient oceanic basin—New evidence from Yining Block of the Carboniferous[J]. *Acta Petrologica Sinica*, 26(10): 2 905 ~ 2 912 (in Chinese with English abstract).
- Li Yongjun, Li Zhucang, Zhou Jibing, et al. 2009a. Division of the Carboniferous lithostratigraphic units in Awulale area, western Tianshan [J]. *Acta Petrologica Sinica*, 25 (6): 1 332 ~ 1 340 (in Chinese with English abstract).
- Li Yongjun, Wang Zuopeng, Li Xinguang, et al. 2018. The discovery of bubble rhyolite in the Early Carboniferous and geochemical characteristics in Yining Block[J]. *Acta Petrologica Sinica*, 34(1): 49 ~ 62 (in Chinese with English abstract).
- Li Yongjun, Wu Le, Li Shuling, et al. 2017. Tectonic evolution of Yining block: Insights from carboniferous volcanic rocks [J]. *Acta Petrologica Sinica*, 33(1): 1 ~ 15 (in Chinese with English abstract).
- Li Yongjun, Yang Gaoxue, Li Hong, et al. 2012. Confirmation of Devonian volcanic rocks from Yining block, Xinjiang and its geological significances[J]. *Acta Petrologica Sinica*, 28(4): 1 225 ~ 1 237 (in Chinese with English abstract).
- Li Yongjun, Yang Gaoxue, Zhang Tianji, et al. 2009b. Definition of the major fold episode Shanshan movement in Yining massif, Western Tianshan Mountains, and it's geology significance[J]. *Advances in Earth Science*, 24 (4): 420 ~ 427 (in Chinese with English abstract).
- Li Yongjun, Zhang Tianji, Luan Xindong, et al. 2008a. Clarification for Late Paleozoic unconformities in the Tekes Daban area of West Tianshan and its geological significance[J]. *Acta Geoscientica Sinica*, 29 (2): 145 ~ 153 (in Chinese with English abstract).
- Liang Q, Jing H and Gregoire D C. 2000. Determination of trace elements in granites by inductively coupled plasma mass spectrometry [J]. *Talanta*, 51(3): 507 ~ 513.
- Liu Ge, Lü Xinbiao, Chen Chao, et al. 2014. Zircon U-Pb chronology and geochemistry of Mesozoic bimodal volcanic rocks from Nenjiang area in Da Hinggan Mountains and their tectonic implications[J]. *Acta Petrologica et Mineralogica*, 33(3): 458 ~ 470 (in Chinese with English abstract).
- Liu Xiaoming, Gao Shan, Yuan Honglin, et al. 2002. Analysis of 42 major and trace elements in glass standard reference materials by 193nm LA-ICP-MS [J]. *Acta Petrologica Sinica*, 18 (3): 408 ~ 418 (in Chinese with English abstract).
- Macdonald R. 1987. Quaternary peralkaline silicic rocks and caldera volcanoes of Kenya[J]. *Geological Society London Special Publications*, 30(1): 313 ~ 333.
- Meng En, Liu Fulai, Liu Pinghua, et al. 2014. Petrogenesis and tectonic significance of Paleoproterozoic meta-mafic rocks from central Liaodong Peninsula, northeast China: Evidence from zircon U-Pb dating and in situ Lu-Hf isotopes, and whole-rock geochemistry[J]. *Precambrian Research*, 247(1): 92 ~ 109.
- Meschede M. 1986. A method of discriminating between different types of mid-ocean ridge basalts and continental tholeiites with the Nb-Zr-Y diagram[J]. *Chemical Geology*, 56(3 ~ 4): 207 ~ 218.
- Pearce J A. 1983. Role of the sub-continental lithosphere in magma genesis at active continental margins[A]. Hawkesworth C J & Norry M J. *Continental Basalts & Mantle Xenoliths*[C]. Nantwich: Shiva, 230 ~ 249.
- Pearce J A, Harris N B W and Tindle A G. 1984. Trace element discrimination diagrams for the tectonic interpretation of granitic rocks[J]. *Journal of Petrology*, 25(4): 956 ~ 983.
- Pearce T H, Gorman B E and Birkett T C. 1977. The relationship between major element chemistry and tectonic environment of basic and intermediate volcanic rocks[J]. *Earth and Planetary Science Letters*, 36: 121 ~ 132.
- Qian Qing, Gao Jun, Xiong Xianming, et al. 2006. Petrogenesis and tectonic settings of Carboniferous volcanic rocks from north Zhaosu, western Tianshan Mountains: Constraints from petrology and geochemistry[J]. *Acta Petrologica Sinica*, 22(5): 1 307 ~ 1 323 (in Chinese with English abstract).
- Qiu Jiansheng, Wang Dezi and Zhou Jincheng. 1999. Geochemistry and petrogenesis of the Late Mesozoic bimodal volcanic rocks at Yunshan Caldera, Yongtai County, Fujian Province[J]. *Acta Petrologica et Mineralogica*, 18(2): 97 ~ 107 (in Chinese with English abstract).
- Sun S S and McDonough W F. 1989. Chemical and isotopic systematics of oceanic basalts: Implications for mantle composition and processes[A]. Saunders A D and Norry M J. *Magmatism in the Ocean Basins*[C]. Geological Society of London, Special Publications, 42: 313 ~ 345.

- Tang G J, Chung S L, Wang Q, et al. 2014. Petrogenesis of a Late Carboniferous mafic dike-granitoid association in the western Tianshan: Response to the geodynamics of oceanic subduction[J]. *Lithos*, 202~203(4): 85~99.
- Tang Gongjian, Wang Qiang, Zhao Zhenhua, et al. 2009. LA-ICP-MS zircon U-Pb geochronology, element geochemistry and petrogenesis of the andesites in the eastern Taerbiese gold deposit of the western Tianshan region[J]. *Acta Petrologica Sinica*, 25(6): 1 341~1 352 (in Chinese with English abstract).
- Tischendorf G and Paelchen W. 1985. Zur Klassifikation von Granitoiden/Classification of granitoids[J]. *Zeitschrift fuer Geologische Wissenschaften*, 13(5): 615~627.
- Vervoort J D and Blachert-Toft J. 1999. Evolution of the depleted mantle: Hf isotope evidence from juvenile rocks through time[J]. *Geochimica et Cosmochimica Acta*, 63(3~4): 533~556.
- Wang Bangyao, Jing Delong, Jiang Changyi, et al. 2016. Geological background and metallogenetic mechanism of the eastern Awulale volcanic-hosted iron metallogenetic belt in the western Tianshan[J]. *Acta Petrologica Sinica*, 33(2): 385~397 (in Chinese with English abstract).
- Wang Bo, Dominique Cluzel, Shu Liangshu, et al. 2009. Evolution of calc-alkaline to alkaline magmatism through Carboniferous convergence to Permian transcurrent tectonics, western Chinese Tianshan [J]. *International Journal of Earth Sciences*, 98(6): 1 275~1 298.
- Wang Bo, Michel Faure, Dominique Cluzel, et al. 2006. Late Paleozoic tectonic evolution of the northern West Chinese Tianshan Belt[J]. *Geodinamica Acta*, 19(3~4): 237~247.
- Wang Bo, Michel Faure, Shu Liangshu, et al. 2008. Paleozoic tectonic evolution of the Yili Block, western Chinese Tianshan [J]. *Bulletin De La Societe Geologique De France*, 179(5): 483~490.
- Wang Q, Wyman D A, Zhao Z H, et al. 2007. Petrogenesis of Carboniferous adakites and Nb-enriched arc basalts in the Alataw area, northern Tianshan Range (western China): Implications for Phanerozoic crustal growth in the Central Asia orogenic belt[J]. *Chemical Geology*, 236(1): 42~64.
- Wang Yan, Qian Qing, Liu Liang, et al. 2000. Major geochemical characteristics of bimodal volcanic rocks in different geochemical environments[J]. *Acta Petrologica Sinica*, 16(2): 169~173 (in Chinese with English abstract).
- Whalen J B, Currie K L and Chappell B W. 1987. A-type granites: Geochemical characteristics, discrimination and petrogenesis[J]. *Contributions to Mineralogy and Petrology*, 95(4): 407~419.
- Williams I S, Buick A and Cartwright I. 1996. An extended of early episode Mesoproterozoic metamorphic fluid flow in the Reynold region, central Australia[J]. *J. Metamorphic Geol.*, 14: 29~47.
- Wilson M. 1989. *Igneous Petrology: A Global Tectonic Approach*[M]. London: Unwin Hyman, 1~466.
- Winchester J A and Floyd P A. 1977. Geochemical discrimination of different magma series and their differentiation products using immobile elements[J]. *Chemical Geology*, 20: 325~343.
- Windley B F, Allen M B, Zhang C, et al. 1990. Paleozoic accretion and Cenozoic reformation of the Chinese Tien Shan Range, central Asia [J]. *Geology*, 18(2): 128.
- Wu Fuyuan, Li Xianhua, Zheng Yongfei, et al. 2007. Lu-Hf isotopic systematics and their applications in petrology[J]. *Acta Petrologica Sinica*, 23(2): 185~220 (in Chinese with English abstract).
- Wood D A. 1980. The application of a Th-Hf-Ta diagram to problems of tectono-magmatic classification and to establishing the nature of crustal contamination of basic lavas of the British Tertiary volcanic province [J]. *Earth and Planetary Sciences Letters*, 50: 11~30.
- Xiao W J, Zhang L C, Qin K Z, et al. 2004. Paleozoic accretionary and collisional tectonics of the eastern Tianshan (China): Implications for the continental growth of Central Asia[J]. *American Journal of Science*, 304: 370~395.
- Yin J Y, Chen W, Xiao W J, et al. 2017. The source and tectonic implications of Late Carboniferous-Early Permian A-type granites and dikes from the eastern Alataw mountains, Xinjiang: Geochemical and Sr-Nd-Hf isotopic constraints [J]. *International Geology Review*, 59: 1~14.
- Yuan Honglin, Gao Shan, Dai Mengning, et al. 2008. Simultaneous determinations of U-Pb age, Hf isotopes and trace element compositions of zircon by excimer laser-ablation quadrupole and multiple-collector ICP-MS[J]. *Chemical Geology*, 247(1~2): 100~118.
- Zhang Qi and Li Chengdong. 2012. *Granite: Implications for Continental Geodynamics*[M]. Beijing: Ocean Press, 5~12 (in Chinese with English abstract).
- Zhang Qi, Ran Hao and Li Chengdong. 2012. A-type granite: what is the essence? [J]. *Acta Petrologica et Mineralogica*, 31(4): 621~626 (in Chinese with English abstract).
- Zhao Leqiang, Qin Feng, Jia Fanjian, et al. 2017. Petrogenesis of Late Paleozoic bimodal volcanic rocks on the southern margin of the Junggar Basin and its geodynamic significance[J]. *Acta Petrologica et Mineralogica*, 36(2): 148~162 (in Chinese with English abstract).
- Zhu Y, Guo X, Song B, et al. 2009. Petrology, Sr-Nd-Hf isotopic geochemistry and zircon chronology of the Late Palaeozoic volcanic rocks in the southwestern Tianshan Mountains, Xinjiang, NW China[J]. *Journal of the Geological Society*, 166(6): 1 085~1 099.
- Zhu Yongfeng, Zhou Jing and Guo Xuan. 2006. Petrology and Sr-Nd iso-

topic geochemistry of the Carboniferous volcanic rocks in the western Tianshan Mountains[J]. Acta Petrologica Sinica, 22(5): 1 341 ~ 1 350(in Chinese with English abstract).

附中文参考文献

- 第五春荣, 孙 勇, 林慈銮, 等. 2007. 豫西宜阳地区 TTG 质片麻岩锆石 U-Pb 定年和 Hf 同位素地质学[J]. 岩石学报, 23(2): 253 ~ 262.
- 高俊, 钱青, 龙灵利, 等. 2009. 西天山的增生造山过程[J]. 地质通报, 28(12): 1 804 ~ 1 816.
- 韩琼, 弓小平, 马华东, 等. 2015. 西天山阿吾拉勒成矿带大哈拉军山组火山岩时空分布规律及其地质意义[J]. 中国地质, 42(3): 70 ~ 86.
- 洪大卫, 王式洸, 韩宝福, 等. 1995. 碱性花岗岩的构造环境分类及其鉴别标志[J]. 中国科学(B辑), 25(4): 418 ~ 426.
- 侯可军, 李延河, 邹天人, 等. 2007. LA-MC-ICP-MS 锆石 Hf 同位素的分析方法及地质应用[J]. 岩石学报, 23(10): 2 595 ~ 2 604.
- 李大鹏, 杜杨松, 庞振山, 等. 2013. 西天山阿吾拉勒石炭纪火山岩年代学和地球化学研究[J]. 地球学报, 34(2): 176 ~ 192.
- 李锦铁, 何国琦, 徐新, 等. 2006. 新疆北部及邻区地壳构造格架及其形成过程的初步探讨[J]. 地质学报, 80(1): 148 ~ 168.
- 李永军, 高永利, 佟丽莉, 等. 2009c. 西天山阿吾拉勒一带石炭系阿克沙克组风暴岩及其意义[J]. 地学前缘, 16(3): 341 ~ 348.
- 李永军, 穆平阳, 庞振甲, 等. 2008b. 西天山特克斯达坂库勒萨依序列埃达克岩的确立及钼找矿意义[J]. 岩石学报, 24(12): 2 713 ~ 2 719.
- 李永军, 胡克亮, 周继兵, 等. 2010a. 西天山伊什基里克山早石炭世火山岩浆作用及其成矿[J]. 地球科学——中国地质大学学报, 35(2): 235 ~ 244.
- 李永军, 金朝, 胡克亮, 等. 2010c. 西天山尼勒克北于赞一带下石炭统阿克沙克组扇三角洲相沉积的发现及意义[J]. 地质学报, 84(10): 1 470 ~ 1 478.
- 李永军, 李甘雨, 佟丽莉, 等. 2015. 玄武岩类形成的大地构造环境 Ta、Hf、Th、La、Zr、Nb 比值对比判断[J]. 地球科学与环境学报, 37(3): 14 ~ 21.
- 李永军, 李注苍, 佟丽莉, 等. 2010b. 论天山古洋盆关闭的地质时限——来自伊宁地块石炭系的新证据[J]. 岩石学报, 26(10): 2 905 ~ 2 912.
- 李永军, 李注苍, 周继兵, 等. 2009a. 西天山阿吾拉勒一带石炭系岩石地层)单位厘定[J]. 岩石学报, 25(6): 1 332 ~ 1 340.
- 李永军, 王祚鹏, 李新光, 等. 2018. 伊宁地块早石炭世球泡流纹岩的发现及地球化学特征[J]. 岩石学报, 34(1): 49 ~ 62.
- 李永军, 吴乐, 李书领, 等. 2017. 伊宁地块石炭纪火山岩及其对构造演化的约束[J]. 岩石学报, 33(1): 1 ~ 15.
- 李永军, 杨高学, 李鸿, 等. 2012. 新疆伊宁地块晚泥盆世火山岩的确认及其地质意义[J]. 岩石学报, 28(4): 1 225 ~ 1 237.
- 李永军, 杨高学, 张天继, 等. 2009b. 西天山伊宁地块主褶皱幕鄯善运动的确立及地质意义[J]. 地球科学进展, 24(4): 420 ~ 427.
- 李永军, 张天继, 朱新东, 等. 2008a. 西天山特克斯达坂晚古生代若干不整合的厘定及地质意义[J]. 地球学报, 29(2): 145 ~ 153.
- 刘阁, 吕新彪, 陈超, 等. 2014. 大兴安岭嫩江地区中生代双峰式火山岩锆石 U-Pb 定年、地球化学特征及其地质意义[J]. 岩石矿物学杂志, 33(3): 458 ~ 470.
- 柳小明, 高山, 袁洪林, 等. 2002. 193 nm LA-ICP MS 对国际地质标准参考物质中 42 种主量和微量元素的分析[J]. 岩石学报, 18(3): 408 ~ 418.
- 钱青, 高俊, 熊贤明, 等. 2006. 西天山昭苏北部石炭纪火山岩的岩石地球化学特征、成因及形成环境[J]. 岩石学报, 22(5): 1 307 ~ 1 323.
- 钱青, 王焰. 1999. 不同构造环境中双峰式火山岩的地球化学特征[J]. 地质地球化学, 27(4): 29 ~ 32.
- 邱检生, 王德滋, 周金城. 1999. 福建永泰云山晚中生代双峰式火山岩的地球化学及岩石成因[J]. 岩石矿物学杂志, 18(2): 97 ~ 107.
- 唐功建, 王强, 赵振华, 等. 2009. 西天山塔尔别克金矿区鞍山岩 LA-ICP-MS 锆石 U-Pb 年代学、元素地球化学与岩石成因[J]. 岩石学报, 25(6): 1 341 ~ 1 352.
- 汪帮耀, 荆德龙, 姜常义, 等. 2016. 西天山阿吾拉勒火山岩型铁矿带东段成矿地质背景与成矿机理[J]. 岩石学报, 33(2): 385 ~ 397.
- 王焰, 钱青, 刘良, 等. 2000. 不同环境下双峰式火山岩的主要特征[J]. 岩石学报, 16(2): 169 ~ 173.
- 吴福元, 李献华, 郑永飞, 等. 2007. Lu-Hf 同位素体系及其岩石学应用[J]. 岩石学报, 23(2): 185 ~ 220.
- 张旗, 李承东. 2012. 花岗岩: 地球动力学意义[M]. 北京: 海洋出版社, 5 ~ 12.
- 张旗, 冉皞, 李承东. 2012. A 型花岗岩的实质是什么? [J]. 岩石矿物学杂志, 31(4): 621 ~ 626.
- 赵乐强, 秦峰, 贾凡建, 等. 2017. 准噶尔盆地南缘晚古生代双峰式火山岩成因机制及其地球动力学背景[J]. 岩石矿物学杂志, 36(2): 148 ~ 162.
- 朱永峰, 周晶, 郭璇. 2006. 西天山石炭纪火山岩岩石学及 Sr-Nd 同位素地球化学研究[J]. 岩石学报, 22(5): 1 341 ~ 1 350.